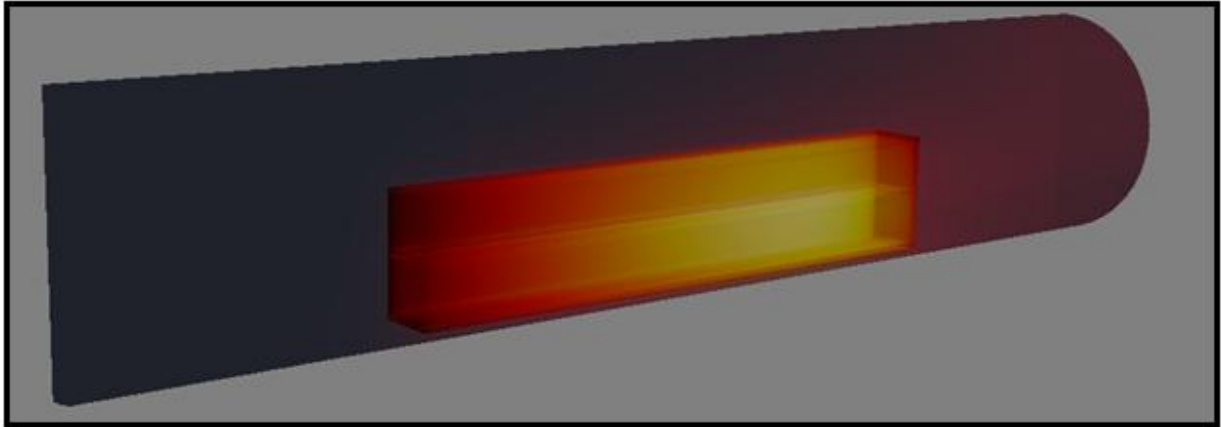


# CHALMERS



## Development of evaporation models for CFD For application within drying process simulation

*Master of Science Thesis*

**SAM E.H. ROBJER GULLMAN**

Department of Chemical Reaction Engineering

Chalmers University of Technology

Göteborg, Sweden, 2010

Report No. xxxx

## Abstract

The objective of this thesis was to develop a method to reliably model the complete process of drying of materials with fluid dynamics software (CFD). The main applications for this are evaporation from porous bodies in industry processes. The modeling included the separate behaviors of the drying periods and was a time dependant process. A number of assumptions were made which allowed the formulation of a model to be implemented using user defined functions in Fluent. The main limitations included in these assumptions were treatment of a porous rigid body and stationary liquid water. Two different approaches were tried, trying to model the constant- and the falling rate periods respectively. In the end the model for the falling rate period was useable for both types of behavior and proved to give reliable results corresponding closely to experimental data. There are possibilities for modifying the final model for application in a wider range of situations.

*Keywords: CFD, evaporation, UDF, drying, water, modeling*

Thanks to:

Prof. Bengt Andersson, *for continuous assistance, involvement and support during the project.*

Ph.D student Andreas Lundström, *for support, help with the UDFs, and the chance to test the model against an advanced case.*

Everyone else at Chemical Engineering Department, Chalmers, *for the welcoming and helpful atmosphere.*

The Coffee Machine, *for being there when I need you.*

## Table of Contents

<b>ABSTRACT</b> .....	<b>2</b>
<b>TABLE OF CONTENTS</b> .....	<b>3</b>
<b>1. INTRODUCTION</b> .....	<b>5</b>
<b>2. PROBLEM DESCRIPTION</b> .....	<b>7</b>
<b>3. THEORY</b> .....	<b>8</b>
3.1 TERMINOLOGY .....	8
3.1.1 <i>Equilibrium Moisture</i> .....	8
3.1.2 <i>Bound &amp; Unbound Moisture</i> .....	9
3.1.3 <i>Types of Materials</i> .....	9
3.2 PERIODS OF DRYING.....	9
3.3 KINETICS .....	11
3.3.1 <i>Surface evaporation</i> .....	11
3.3.2 <i>Body evaporation</i> .....	13
3.4 CFD THEORY.....	15
3.4.1 <i>Fundamental Equations</i> .....	15
3.4.2 <i>Turbulence Models</i> .....	15
<b>4. METHOD</b> .....	<b>17</b>
4.1 TEST CASE.....	17
4.1.1 <i>Geometry</i> .....	17
4.1.2 <i>General Boundary Conditions</i> .....	18
4.1.3 <i>Setup</i> .....	18
4.2 SOFTWARE USED.....	18
<b>5. CONSTANT RATE MODEL</b> .....	<b>19</b>
5.0.1 <i>Applications</i> .....	19
5.1 MODEL DEVELOPMENT .....	19
5.1.1 <i>Assumptions</i> .....	19
5.1.2 <i>Expressions</i> .....	19
5.1.3 <i>Limitations &amp; Problems</i> .....	20
5.2 MODELING.....	21
5.2.1 <i>Validation &amp; Results</i> .....	22
5.3 APPLICATION – FRUIT DRYER .....	24
5.3.1 <i>Presentation</i> .....	24
5.3.2 <i>Modelling</i> .....	24
5.3.3 <i>Results</i> .....	25

<b>6. FALLING RATE MODEL.....</b>	<b>26</b>
6.0.1 Applications.....	26
6.1 MODEL DEVELOPMENT .....	26
6.1.1 Assumptions.....	26
6.1.2 Expressions.....	27
6.1.3 Limitations & Problems .....	28
6.1.4 Geometry and Boundary Conditions .....	28
6.2 MODELING.....	28
6.2.1 Case Results .....	29
6.3 APPLICATION – DRYING OF CATALYST .....	32
6.3.1 Presentation.....	32
6.3.2 Modeling .....	33
6.3.3 Results.....	35
<b>6. DISCUSSION &amp; CONCLUSIONS .....</b>	<b>37</b>
<b>REFERENCES.....</b>	<b>38</b>
<b>APPENDIX .....</b>	<b>39</b>
A.1 RELATIONS.....	39
A.2 – UDF FILES .....	40
A.2.1 Presentation of UDF - Constant Rate .....	40
A.2.2. Presentation of UDF – Falling Rate .....	41
A.3. PRETTY PICTURES .....	42
A.3.1 Test Case Constant Rate .....	42
A.3.2 Dryer Plate Case.....	43
A.3.3 Dryer Baffled Case .....	44
A.3.4 Falling Rate Test Case – Startup .....	45
A.3.6 Catalyst – 100s.....	46
A.3.6 Catalyst – 350s.....	47
A.3.7 Catalyst – 425s.....	48

# 1. Introduction

Traditionally, calculations on industrial equipment in chemical engineering are performed with simplified models of the specific process. It has been difficult to examine in detail the conditions in specific parts of the equipment and engineers have had to rely on their skills and intuition, coupled with experiments to analyze and design plant processes. The methods developed have been largely successful in the creation of equipment and production trains and remain today absolutely necessary for the design of any industrial equipment.

The exponential increase in computational power the last few decades has lifted a number of new methods to the surface. Old and tested methods can be combined to create dynamic simulations of whole process plants, for example. Another 'new' method is the use of CFD, computational fluid dynamics, to directly simulate flows and processes. CFD approximates a domain with a finite number of cell elements, and allows an engineer to visualize the problem in detail by directly solving the equations for flow and transport in these cells. Due to the increased availability of cheap computational power, CFD is moving from its previous place as a tool for research into the area of complex problems and equipment design in the industry. Development of CFD software has resulted in several products, among them FLUENT and CFX<sup>[4]</sup>.

While the software enables an engineer to solve flows and reactions for a design, it is required of him or her to provide the correct models and data. CFD has largely been used to model different types of gas flows, for the design of airplanes and cars. Therefore the largest part of its development has been in the areas of laminar and turbulent flows, and the development of methods to accurately simulate and model these flows. As a design tool for chemical equipment it has not seen as much development, and is still adapting. For the design of any chemical process with CFD, reliable models are needed to model the chemical reactions and interactions.

The possibilities when using CFD to design industrial equipment are many, and the utility of including CFD in the development process gives rise to more specific design opportunities as well as provides new methods of validation. A simulation may include chemical reactions, and transfer of heat and mass along with the flow simulation. This lets the designer check for things such as optimal injection points, flow patterns for maximum heat transfer and validation of previous simplifications and assumptions in the models used.

One of the areas where CFD will prove useful is in the simulation of evaporation of water, or drying. As one of the most common separation processes it is present in the food industry, textile industry, paper industry and many others. The process is well known and the study of drying has provided a large number of models and designs for comparison of results. However the implementation of CFD in evaporation problems is still rather limited<sup>[8]</sup>. Development of standard methods to solve the problems of evaporation is therefore needed, this will be the focus of this thesis.

The types of problems that arise when dealing with evaporation are in many cases quite complex. It is often possible to simplify the problems a great deal if one is interested in the overall process, such as the effectiveness of a dryer. However if the goal is to study the drying of an isolated body and see the differences and effects on the drying process in different areas of the problem will be increasingly complex. It will most likely require a number of simplifying assumptions, especially since all detail cannot be resolved due to the differing length-scales of the process.

The evaporation process is interesting in many different situations, and the type of information needed may require different approaches to it. Depending on the limiting step in the process, different ways to model it may be appropriate. In some cases the evaporation from a surface is the interesting step in a process, such as the estimation of the efficiency of different dryer geometries. In others the level of water in different regions of a porous body will be important, such as when checking that the material in the dryer is dried evenly in all regions. This is important for clay burning and fruit drying processes, among others<sup>[10][11]</sup>.

By using numerical simulation it will be possible to further optimize previous designs of equipment, and provide more effective equipment to the industry. As an example of how this can be done this thesis will detail different types of processes and how one might simulate them with CFD. The lessons learned from this will hopefully provide ideas for the development of similar methods for other applications.

## 2. Problem Description

When treating drying with numerical simulation a number of different issues arise. As will be described in the theory section below the process of drying consist of several stages, interaction between different phases and a large spectrum of time scales.

The *time scale* problem is probably the most complex one to solve. A drying process can stretch over several hours for drying of dense and wet materials. However the reactions take place very quickly, the two mechanisms of evaporation and condensation are extremely fast, and most of the time only the difference between them can be observed and is often termed the drying rate. When performing numerical simulation this becomes a problem since not only space but time is discretized and the time step chosen needs to be sufficiently small so that everything is resolved correctly. A too large time step will result in calculation error, and in this case a large overestimation of the reaction rate with a divergent solution as result. Since choosing a very small time step will result in vastly increased computational times the modeling of a whole drying process will be an extremely arduous process, if at all possible.

The *phase interaction* between liquid water and water vapor, between water contained within the material and water on the surface would require a lot of factors to be taken into account if they need to be resolved in detail. There are CFD models for multiphase flows that keep track on liquid-gas surfaces and are able to model the interaction between them, they are however not suited for this type of situation and are not suited to describe liquid contained within a solid object. It could be possible but could again require too much computational effort to be of any real use for real applications.

The third problem of *stages of drying* arises when treating the whole drying process. In reality drying of an object is divided into several periods with very different behavior which means that a model or method must be able to describe all of these behaviors and can as a result not be too simplified. It could be possible to divide the method into several models, one for each period but this would not be the preferred solution.

### 3. Theory

If studied in detail, evaporation is a complex process with a large number of factors. A simple case is evaporation from a water body in motionless air. It can be convenient to regard some processes to be similar to this case, and the study of it can be of help when developing models for more complex cases. For industrial purposes the processes involved are often much more complex, such as the drying of food products. This situation can have internal and external diffusion, a gradually changing shape of the body and constants that change with temperature and water content. To produce a model for cases like this, it is important to describe in detail how the process takes place.

#### 3.1 Terminology

For the treatment of evaporation problems, a number of useful variables can be defined. These terms will be used throughout the report and will be presented thoroughly here. <sup>[1][3][2]</sup>

When dealing with the drying of bodies it is common to define the terms ‘moisture content’ and ‘humidity’. Moisture content  $X$ , is the mass fraction of water ( $M_w$ ) to solid ( $M_s$ ) in a solid body or object. It is used to track the level of moisture in the area of interest, and has a fixed point of reference. Related to  $X$  is  $W$ , the moisture fraction. It is the fraction of moisture mass to total mass of the object.  $W$  is useful because it only ranges between 0 and 1, whereas  $X$  can range to infinity. For a gas we can define the humidity  $Y$ . This is the fraction of water vapor mass ( $M_v$ ) to mass of the dry (vapor free) gas ( $M_g$ ).

$$\text{---} \quad (3.1)$$

$$\text{-----} \quad (3.2)$$

$$\text{---} \quad (3.3)$$

$$\text{---} \quad (3.4)$$

Further it is convenient to define expressions for the level of moisture in air relative to its maximum possible value. Water vapor has a maximum partial pressure in air of a given temperature and pressure, for which the gas is said to be saturated with moisture. This pressure is defined as  $P_o$ . We can define a relative humidity  $\psi$ , which is the ratio of the current water vapor pressure ( $P_v$ ) to its maximum value. This is a useful measure of the evaporation potential of the air.

$$\text{---} \quad (3.5)$$

##### 3.1.1 Equilibrium Moisture

When a wetted object is in equilibrium with the surrounding air, at constant  $T$ ,  $P$  and humidity the moisture left in the object is said to be the equilibrium moisture content. When using the dry basis moisture content,  $X$ , one might define the equilibrium moisture as  $X^*$ . The difference between the current moisture content and  $X^*$  is called the free moisture  $X_f$ . This is the amount of moisture that can be released before the system reaches its equilibrium and is an important term since it can be seen as a driving force for the evaporation. <sup>[1]</sup>

$$(3.6)$$

$$\text{---}$$

$$(3.7) \text{ } ^{[1]}$$

According to Keey <sup>[1]</sup> the dependence on the equilibrium moisture content with temperature can be correlated by the above expression.  $\alpha$  is said to vary between 0.005 and 0.01 (1/K).



### 3.1.2 Bound & Unbound Moisture

When contained inside a porous material, a liquid can be said to be unbound or bound. The unbound liquid behaves like free water and is not adsorbed in any way to the material. The bound moisture is characterized by an adsorption heat, and a lower enthalpy state. The adsorbed water will require additional heat to be able to be evaporated. This heat of wetting may be approximated (according to Smith and van Ness<sup>[3]</sup>) by assuming that the vapor phase behaves as an ideal gas and that the volume of the condensed phase is negligible compared to that of the vapor phase. Then one might use the equation below. Typical values of  $\Delta H_w$  range between 100 j/mol and 5000 j/mol<sup>[1]</sup>.

$$\text{--- (3.8) } \quad \text{---} \quad \text{--- (3.9) }^{[1]}$$

A solid object containing bound water, and in equilibrium with its surroundings, will exert a vapor pressure that is lower than the saturation pressure at a set temperature. We define the activity A as the ratio of the vapor pressure of the bound water to that of a free water surface. The value of A depends primarily on the size of the pores in the solid material, which will lower the exerted vapor pressure. Smaller pores will have the effect of more difficult transport and a lower activity.

In reality there are three main types of bound water. Water can be located in small pores, which will make it more difficult to evaporate since the pores will lower the possible vapor pressure to be exerted by the gas according to []. It can also be adsorbed onto a surface, a state which has an additional enthalpy in the range of 1-10 kJ/mol. Finally, water can be chemisorbed to a surface, meaning attached by chemical bonds. This will give an added enthalpy of >10 kJ/mol.

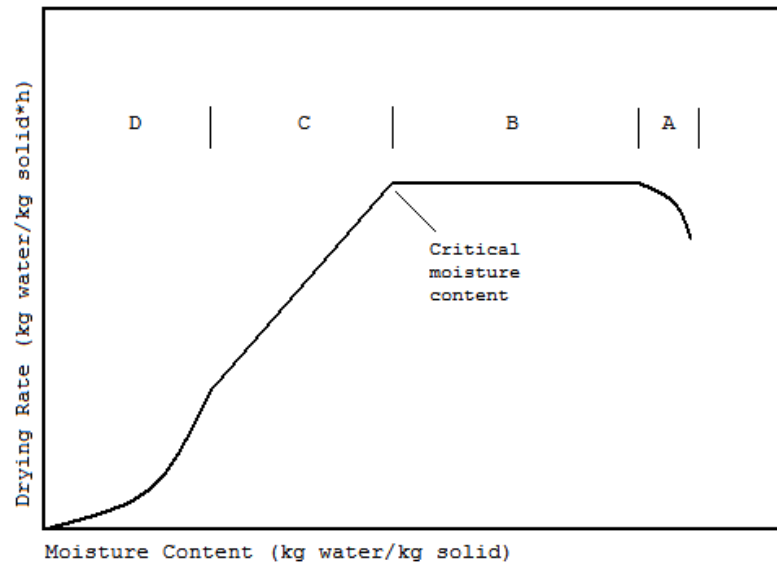
### 3.1.3 Types of Materials

According to Faust<sup>[3]</sup>, solids consist of two main types with regard to their drying behavior. The first type is mostly inorganic matter, like sand, clay and catalyst material. These hold moisture in open spaces between solid particles with little to no ability to absorb moisture into the material, thus most of the moisture is unbound. These solids can be dried relatively quickly and it is possible to reach very low moisture contents.

The second types of materials are mostly organic, like fruit, wood and food products. These have in common that they all have an ability to bind moisture, significantly elevating the equilibrium moisture content for a given set of drying conditions. Because of the bound moisture, drying of these materials is much more energy demanding. It is only possible to dry these materials to low moisture contents with a very dry gas.

## 3.2 Periods of Drying

The process of drying a wet body from the initial heating of the body to its finished dry state consists of several periods with varying conditions. The process is divided into periods, where each period has a separate behavior. When regarding the rate of drying in an industrial dryer, one can commonly identify four periods. The length, and even existence of these periods will depend on the material being dried



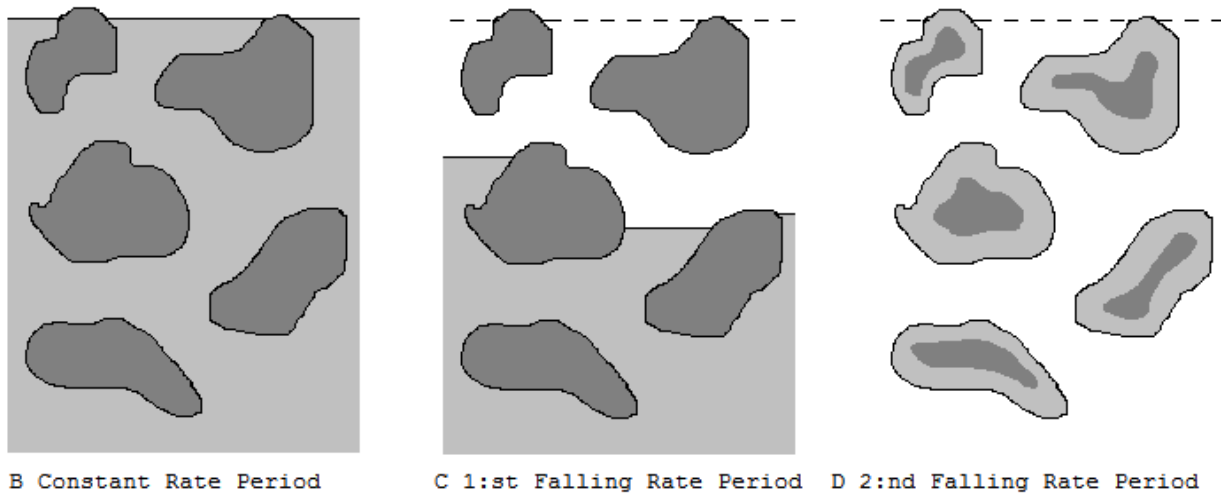
Picture 3.1 – Periods of Drying

and the conditions under which the drying occurs. The moisture content when the rate of drying starts to decrease is called the critical moisture content,  $X_c$ .<sup>[3]</sup>

The first period (A) is the heating period, when the dry object is cold and is slowly warmed up by the circulating air. The limiting process in this period is the heat transfer to the body from its surroundings. As the body gets heated, water will start to evaporate and after a short while it will reach a steady state. This is the start of the second period (B) which is called the constant-rate period. During this period the transport of heat to and the evaporation from the body are at steady-state which gives a constant evaporation rate. It has been observed that during this period the surface of the material is at a uniform temperature. This temperature is named the wet-bulb temperature, and varies with temperature and initial humidity of the surrounding air. This is well documented and the wet-bulb temperature can be found from humidity charts.

During periods A and B, the evaporation takes place at the surface of the material. There is no internal resistance to mass transfer and the conditions are very similar to that of evaporation from a free water surface. The larger cavities within the material are filled with liquid water and particles or cells are wetted. When most of the easily accessible water has been evaporated the process reaches the point

named the critical moisture content, and period C starts.



Picture 3.2 – Visual depiction of drying mechanisms

The third period, called the first falling rate period (C) will give a constantly decreasing drying rate. This is because the moisture is now retreating beyond the immediate surface of the object, making it more difficult for the moisture to evaporate. The area of evaporation is significantly lowered resulting in a constantly lowering evaporation rate. Diffusion of the water vapor inside a material is the limiting step in this period, and as the diffusion path increases the rate of drying will decrease linearly. The last period, if it exists, is a second order process. When most of the easily accessible water in a body is depleted the drying enters the second falling rate period (D). The rate in this period falls rapidly with moisture content. The period is limited by diffusion of liquid water within a body or grain. The type of diffusion depends on the material being dried. It is possible to have a period D by drying a material with large differences in particle size but no ability to absorb moisture. This is because the material will be dried in larger channels first, and the presence of many smaller particles creates very small crevices for moisture which will be more difficult to dry creating a diffusion controlled process. In a material where a large amount of bound moisture is present, it is the diffusion of moisture to the particle surface that is the limiting step.<sup>[3]</sup>

### 3.3 Kinetics

We have concluded that a drying process can be divided into several types of behavior, depending on the rate-controlling mechanism. To be able to model the evaporation correctly one needs knowledge of the type of evaporation that takes place. This section will describe briefly the mechanisms of the constant-rate period and the falling rate periods respectively.

#### 3.3.1 Surface evaporation

For the constant rate period, evaporation takes place directly from the free water at the surface of the body. It is assumed that all resistance to heat and mass transfer takes place in the surrounding air film, and that the object itself has a constant temperature. Under these conditions we know that the mass transfer and heat transfer are in equilibrium and take place at a constant rate.<sup>[1][2][5]</sup>



(3.12)

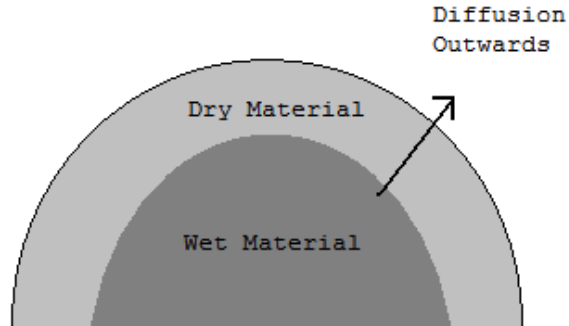
Where the mole fraction difference between the surface and the edge of the boundary layer divided by the boundary layer thickness gives a linear gradient. This may also be expressed by the above formulation where the gradient is expressed in partial pressures of water vapor. This form is useful since it can be assumed that the vapor pressure at the surface is the same as the saturation pressure for water vapor at the corresponding temperature.

Similar expressions have been used to estimate surface evaporation in dryer design, although more refined.

### 3.3.2 Body evaporation

When drying enters the falling rate period of drying, diffusion inside the body will be the limiting process. The diffusion path of the water will change with time, and a larger diffusion distance will mean a lower rate of drying. This behavior can be seen in almost all types of materials during drying and although the type of transport may differ between gas diffusion, liquid diffusion and capillary action, the general effect is similar. <sup>[3][5]</sup>

As the last water at the surface evaporates, the body will start to heat above the wet-bulb temperature and heat will be transported into the body by conduction. If the material is porous it is possible for water to evaporate inside the channels of the material and diffuse to the surface. If the material has very small pores or if the water is bound inside cells or fibers the water will diffuse in liquid form first, in some cases all the way to the surface, before evaporating. To properly model this process will be different from that of the surface evaporation. First of all it is time-dependent, and a steady state solution does not exist. Second, the inside of the body will need to be included in the process, and the water contained there will need to be dealt with.



Picture 3.4 – Diffusion during falling rate period

When water is removed from the body there will be changes in a number of material properties. Changes in the heat capacity, density and heat conductivity will all need to be accounted for. They will be varying with moisture content  $X$  of the material. Depending on the mechanisms involved it is possible that the effective diffusivity of moisture will change with  $X$  as well. In many real cases, especially involving materials of type 2, shrinkage of the body will occur as water is removed from it. This is difficult to simulate directly for any geometry other than very simple ones. <sup>[2][5]</sup>

The actual evaporation process will depend on the material being dried and the processes involved. For the purpose of this project we will consider a simplified case, where many of the complexities can be ignored. This is the drying of a rigid and highly porous body, with large pores and no bound water. The liquid water is located in pores and channels, and the material itself is dense enough so that no diffusion of liquid water takes place in it, only heat transport. If this is the case we can make a number of assumptions that will make modeling of the process simpler:

- All water transport takes place by diffusion of water vapor.
- All liquid water can be treated as stationary, and unbound.
- The body will not change shape due to decreasing moisture content.

The material properties of this material can be estimated by weighing them between water and the solid material, and there are different ways of doing this. The way chosen will be presented during model development.

### 3.4 CFD Theory

Computational fluid dynamics is a way to obtain flow and pressure profiles for flows of different types by numerical computation. As a tool it is very flexible, although in many areas dependant on models for different phenomenon such as turbulence or particle tracking. The computational domain, that is the actual geometry of interest, needs to be provided by the user in the form of a 'mesh'. The mesh consists of the geometry divided into a large number of sub-cells for which the software is able to solve the fundamental equations for the flow. The solution of the problem is highly dependent on that the mesh is detailed enough to avoid larger computational errors, since the real flow is approximated by a finite number of data points. <sup>[4]</sup>

#### 3.4.1 Fundamental Equations

The Navier-Stokes equations commonly used to describe flow are derived for a finite computational cell and solved in the form of the momentum equations (3.13) and the continuity equation (3.14). If the flow can be treated as non-compressible, the equations can be significantly simplified by setting  $\rho$  constant.

$$\rho \left( \frac{d\mathbf{u}}{dt} + \mathbf{u} \cdot \nabla \mathbf{u} \right) = -\nabla p + \nabla \cdot \boldsymbol{\tau} + \mathbf{f} \quad (3.13)$$

$$\nabla \cdot \mathbf{u} = 0 \quad (3.14)$$

After solving the momentum equations the continuity equation is often unfulfilled and pressure-velocity relationship needs to be solved iteratively. For example by using the equation below, for flows with constant density and viscosity.

$$\nabla^2 p = \nabla \cdot \left( \rho \mathbf{u} \cdot \nabla \mathbf{u} \right) - \nabla \cdot \mathbf{f} \quad (3.15)$$

For solving the species interaction when having multiple species one uses the following equation(s):

$$\frac{d\mathbf{u}_i}{dt} + \mathbf{u}_i \cdot \nabla \mathbf{u}_i = -\nabla p_i + \nabla \cdot \boldsymbol{\tau}_i + \mathbf{f}_i \quad (3.16)$$

Kinetic, thermal and chemical energy does not have a strong coupling with the momentum equations for incompressible flows. They can be solved separately. The equation for thermal energy is formulated for a cell the following way:

$$\rho c_p \left( \frac{dT}{dt} + \mathbf{u} \cdot \nabla T \right) = \nabla \cdot \mathbf{q} + \dot{q} \quad (3.17)$$

Again, if  $\rho$  and  $c_p$  can be taken constant, the equation can be simplified.

#### 3.4.2 Turbulence Models

To solve the chaotic nature of turbulent flows, many types of models exist to be chosen from. The more computationally efficient of these models treat turbulent flow as isotropic and make use of two additional equations to describe the new properties of the flow. The most common is the k- $\epsilon$  model

which introduces the turbulent kinetic energy ( $k$ ) and the energy dissipation rate ( $\epsilon$ ) and solves transport equations for these properties.

If the flow has high turbulence, the grid resolution close to the wall is often unable to resolve the wall interaction the normal way, by using the no-slip condition. In these cases wall functions need to be used to model the wall interaction effects. The wall function models the viscous effects close to the wall. A scaled variable called the  $y^+$  value is used to determine if wall functions need to be applied. In general a value of 30 or above requires wall functions since the boundary layer is fully turbulent. <sup>[4]</sup>



## 4. Method

Models will be explored for two cases. The first one will try to model the constant rate period with a steady state solution, while the second will depict the transient case of the falling rate period. In both cases a UDF will be tied to Fluent to allow for a high level of control. For both cases an initial model idea will be discussed and tested on a simple geometry, to see if the general sought-after behaviors can be identified and adjusted according to need. A simple geometry also makes it possible to compare the results to known correlations for validation of the models.

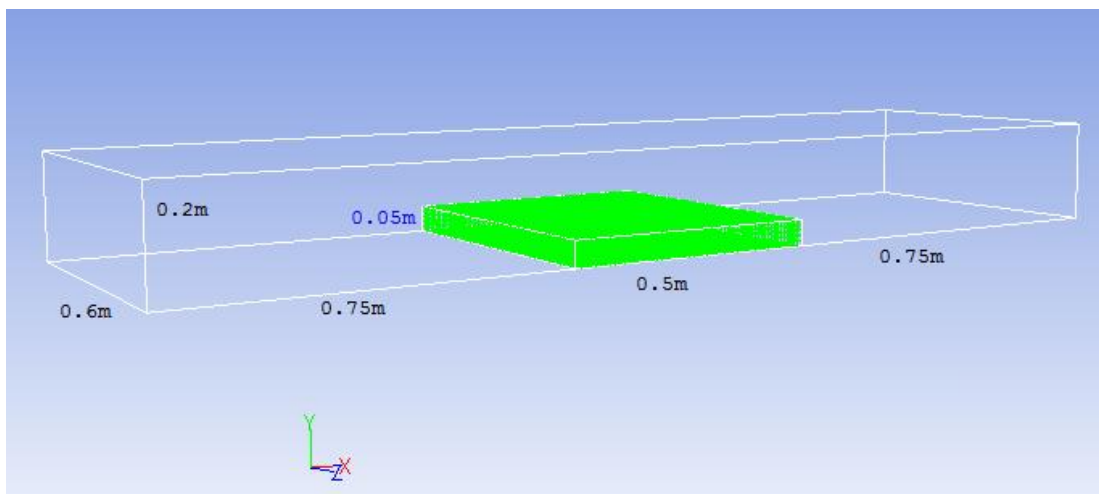
The test run is followed by an applied run on a more realistic case, to evaluate the usefulness of the models. The set-up for the test case will be described in detail below. The advanced cases, however, will not since this would require too much space.

### 4.1 Test Case

#### 4.1.1 Geometry

The geometry used for the testing of the model is very simple. A flat plate is placed in a square channel, the plate is quite thin and the hot air will flow above it. The plate will only allow evaporation and heat transfer from its top surface, not the sides. This makes correlations more accurate and provides one dimension of diffusion for the falling rate model.

The dimensions of the channel are 0.6x0.2x2m. The dimensions of the plate are 0.6x0.5x0.05m. Evaporation will take place from the surface only. The plate will be modeled as a porous zone and no flow will take place in it.



Picture 4.1 – Test mesh geometry outline

The mesh detail is deemed very important close to the surface, to justify the assumptions made. A boundary layer is chosen with increasing cell thickness outwards where the initial cell thickness is 0.5mm. The boundary layer will be varied later on, so several meshes will be created based on this geometry. In total the mesh will have 255000 cells.

### 4.1.2 General Boundary Conditions

In the initial case the air will flow in the channel with an inlet velocity of 1 m/s and a temperature of 343K. Due to compression of the channel the air will have an average velocity of 1.33 m/s over the plate.

Thus the inlet conditions will be:

$$v_{in}=1 \text{ m/s}$$

$$T_{in}=343 \text{ K}$$

### 4.1.3 Setup

The flow will be turbulent with a Reynolds number of 13000, thus a turbulence model is needed. The k- $\epsilon$  model is chosen, and the conditions for k and  $\epsilon$  in the inlet will be provided by the means of hydraulic diameter and turbulent intensity.

## 4.2 Software Used

Below all the software used during this project is presented.

- ANSYS Fluent 12.1.4 was used to perform CFD simulations, and compilation of UDF files.
- Meshing was done with GAMBIT and ANSYS Meshing application.
- MATLAB was used for data processing and graphs.
- ParaView was used for data post-processing for the Fluent data files.
- Microsoft Visual C++ was used for programming of the UDF files.
- The Microsoft Office package was used for report, tables and presentation material.
- Good old MS Paint was used with affection for certain diagrams and picture processing.

## 5. Constant Rate Model

The development of a model for the constant-rate drying period will be based on the theoretical background given in 3.3.1. By using user defined functions it is possible to choose the type of model with greater flexibility than by using the fluent interface. The model will need to correctly estimate the evaporation flux from a surface and be stable enough for fluent to find a solution.

### 5.0.1 Applications

Possible applications include efficiency screening of drying equipment, and examination of conditions that affect the drying outside of the object being dried.

## 5.1 Model Development

Here a presentation on the theory used will be supplied. A model for the constant rate of drying will be useful when designing drying equipment and other processes which need to take into account wet surfaces and evaporation effects. Any material where internal transport of moisture is fast and surface conditions remain constant can be effectively modeled by a constant rate expression<sup>[3]</sup>. The most important quality of the model should be to take into account the effect of convective flow on or over the surface where evaporation will occur.

### 5.1.1 Assumptions

The assumptions made in the model are based on the observed behavior of the constant-rate drying period. It is assumed that, first of all, a steady state solution exists. As has been observed during drying processes this corresponds well to reality but will still be an approximation. It is assumed that the liquid water and the evaporated water are in equilibrium at the surface of the body, and that there is no transport of moisture within the body itself. The water at the interface is considered unbound, and thus exert a vapor pressure equal to that of a free water surface, with corresponding enthalpy difference between liquid and vapor. The body is assumed to have a very high conductivity, to be able to find a solution where it is easy to find the correct behavior at the wet-bulb temperature.

Further, it is assumed that a boundary layer of stagnant gas exists, and that the process is entirely limited by the diffusion in that film. There is only heat transfer through the gas, and no radiative heat transfer is taken into account. The gradient in the expression for diffusion is approximated by a linear gradient over the boundary layer, and the boundary layer is assumed to have a certain thickness.

Heat of evaporation and diffusivity are assumed constant, as are any heat capacity values.

### 5.1.2 Expressions

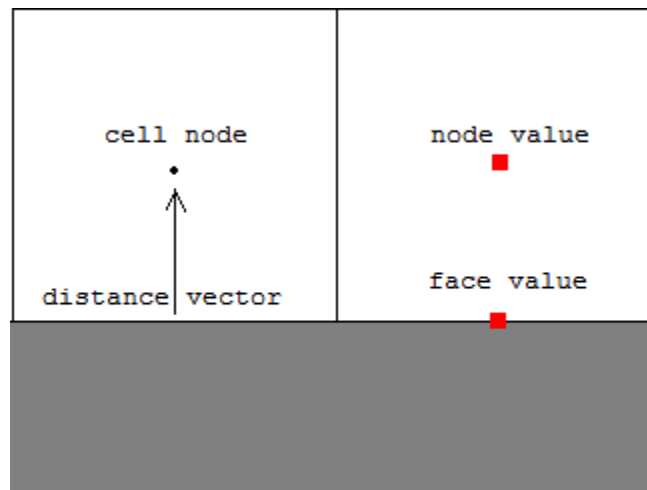
Evaporation takes place at the surface, and the vapor will diffuse outwards. The reaction expression will describe the initial diffusion through a fictive boundary layer, and will be modeled as a source term in Fluent. This will give the solver information about evaporated or condensed water and modify the solution accordingly. The reaction expression is a modified form of 3.12 where two new factors are introduced.

$$\text{---} \quad \text{---} \quad \text{---} \quad \text{---} \quad (5.1)$$

The factor  $k_c$  is used in the iteration process to adjust the reaction rate for the specific solution. It will in a crude way represent a diffusivity adjustment, turbulent or molecular. In the ideal laminar case, with the correct value of  $k_c$  it should be 1. It is a fast way to make a change to the overall reaction rate if need be. The factor  $k_c$  is an adjusting factor since fluent expects a volumetric reaction rate. This factor will multiply the rate by the face area in a cell where evaporation takes place and divide by the total cell volume to arrive at the right units for the expression. It is also needed to correct the expression for the assumption that the boundary layer is of a certain thickness. To find the correct saturation vapor pressure for the above expression, a tested expression is used. The Goff-Gratch expression for vapor pressure can be found in appendix A.1.

The partial pressure at the edge of the boundary layer is taken at the central node for the cell where evaporation takes place, and the boundary layer thickness will be the distance between this cell node and the cell surface where evaporation is set to occur. Thus the gradient will be approximated by the value within a single cell, and it is important that the assumptions made about the boundary layer are correct within this cell. This will be done for all cells where evaporation will occur. It is important to note that this assumption puts large restrictions on the mesh used, since the cell closest to the surface should closely resemble the boundary layer in thickness. Since the boundary layer thickness will vary it is almost impossible to meet this criterion, but this assumption is taken as a first estimate.

If the cell thickness is not close to that of the boundary layer the user needs to correct for that by changing  $k_c$  later.



Picture 5.1 – The surface cell gradient

### 5.1.3 Limitations & Problems

The limitations of this model are several. It relies on the existence of constant conditions to be able to find a steady state solution. If one wishes to model the depletion of water or any other time dependent process this is not possible. The assumptions made about equilibrium at the surface and the boundary layer puts further limitations on its usefulness, since it will be very hard to model thin, or varying boundary layers such as with impinging flows and high flow rates. The gradient over the boundary layer

is assumed to be constant in a cell, which in reality it is not. This will prevent the model from achieving high-accuracy results.

## 5.2 Modeling

Modeling this problem will be a little tricky. By entering the right values for reaction constants and running, the solver will most likely diverge and never find the steady state solution required. The modeling will need to be taken in careful steps, to give the next batch of iterations a good starting point, gradually changing the solution until it gives good results. The ease with which this happens will depend to a large extent on the problem geometry presented and the mesh.

A number of different meshes were tried for this problem, and if the solution needs to be such that there are large differences on values of water vapor concentration it will be increasingly difficult to find it. Therefore evaporation is chosen to take place from only one surface, normal to the flow direction to give a good convective flow for the vapor.

Modeling starts with solving for the flow field, thus excluding the energy and species equations. The flow will be turbulent, modeled with the k- $\epsilon$  model so equations for flow, k and  $\epsilon$  are solved for a flow field. The solution is deemed adequate when reaching a residual value of  $1e-4$  for all equations. If large  $y^+$  values are observed, one will need to enable wall functions. This was not the case for the test case, because of the detailed boundary layer.

Next, the equations for energy and species are enabled and the flow equations disabled. The reaction rate for evaporation is set to a value much lower than the real value, allowing the solver to find a solution. At a residual value of  $1e-4$  the solver is stopped and the reaction rate of the evaporation is adjusted upwards before solving again. This process is done until the body reaches its wet-bulb temperature under current conditions. This is because the wet-bulb temperature should be the temperature for when the model resembles reality, and thus it gives a target temperature for the simulation.

Now the solution is closing in on the real steady state solution and in the last step all equations are enabled, to let them converge to a residual value of  $1e-6$  or lower. After this the solution is saved and the process complete.

A number of problems can arise while doing this; the most common is a divergent solution. Often this will happen because of a too large increment in the reaction rate change. One needs to save the data file in each step and if this happens go back and try a smaller reaction rate change. Another common problem is that the solver crashes or gives a warning due to the temperature decreasing below 1K. This is a form of unphysical solution that happens when the solver overestimates the reaction rate. It is important to have a detailed mesh close to the evaporating surface. It is also important to have a fine boundary layer at the surface. When getting close to the real reaction rate one might get oscillating residuals, this can usually be fixed by using slight under-relaxation on the species equation(s), and when the solution is stable changing back to a value of 1 for under relaxation. This gives better convergence at this state.

### 5.2.1 Validation & Results

Tests were run for five cases, varying the thickness of the boundary layer at the surface, and the temperature of the inlet air. It is important to see how the difference in the boundary layer will affect the solution.

	Cell Th	T <sub>in</sub>	ΔT	R <sub>corr</sub>	R <sub>mod</sub>	K <sub>c</sub>	V <sub>cell</sub>
Units	mm	K	K	kg/h	kg/h	35	m/s
Case 1	0.25	343	47.6	0.46	0.62	35	0.12
Case 2	0.5	343	47.8	0.47	0.46	42	0.12
Case 3	1	343	47.4	0.46	0.53	50	0.16
Case 4	0.5	360	59.4	0.57	0.54	25	0.12
Case 5	0.5	330	36.1	0.35	0.35	54	0.12

Table 5.1 – Case Summary

To obtain a measure of the validity of the model, a correlation was used to find the theoretical evaporative flux. Because of the simplified geometry it was possible to use a correlation for a flat plate, to obtain the overall heat transfer coefficient  $h$ . Then equation 3.10 was used to estimate the flux.

$$(5.2)^{[3]}$$

$G$  is the mass velocity in  $\text{kg}/\text{m}^2$ . All values are known from the geometry and inlet conditions. The value of  $h$  was obtained as  $h=21.14$  [ $\text{W}/\text{m}^2\text{K}$ ].  $G = [2450 \ 29300]$   $T=[45 \ 150]^\circ\text{C}$ . The first three cases were run to examine the effect of the boundary layer, and as expected the result will heavily depend on the cell thickness. We can see that for a boundary layer of 0.5mm the model is able to predict the evaporation very well, but only moderately so if the boundary layer differs from this value. This is believed to be because of the first order approximation of the concentration gradient. As is the case now, half of the boundary cell thickness approximates the real boundary layer thickness. If a second order gradient could be obtained, then it is likely that the model would show more mesh independence. The surface boundary layer also had a significant impact on how easy it was to avoid the divergence problem; the more detailed meshes were easier to obtain a solution with. If this model is to be used for more advanced calculations it will need to be calibrated and checked first.



Picture 5.1 – Evaporation of water (red) from object surface

The wall  $y^+$  values were in the allowed range for the plate ( $<5$ ). The wall interaction with the top of the channel gave a maximum of  $37 y^+$ , but this interaction is not deemed to affect the evaporation in any way. We can see some variation in the reaction constant, it was used to adjust the reaction rate towards its real value and different mesh conditions had an impact on the constant. This is natural since the change in cell thickness will strongly affect the first order gradient and some adjustments will be necessary to close in on a realistic value again. The last column shows the velocity of air in the surface boundary cell, it is much higher than would be allowed with the assumptions made of zero velocity. However this could explain the large values of the  $K_c$  constant. The real boundary layer thickness is probably much smaller, which would create a larger gradient. Thus  $K_c$  needs to compensate for the lack of that gradient. It is hard to draw any conclusions about how the cell velocities affect the model results.

By deciding that the 0.5mm mesh was a good option for this particular case, another two tests were performed. This time to see what a change in inlet temperature would have on the model results. The solution was again adjusted with  $K_c$  so that the plate obtained its wet-bulb temperature and theoretical fluxes obtained with the correlation. Over the span of 60K the model was able to predict the evaporative flux very well with changing temperature, as long as the constant is allowed to change to compensate. This shows possible usefulness in tweaking the drying conditions of a process once the model has been calibrated against the geometry used.

At this point the basic model is deemed functioning, and parts of it will be used to develop the more advanced falling rate model. However it has shown a number of problems, such as heavy mesh dependence and difficulty to obtain convergence. These could be more severe in an advanced geometry.

See appendix A.3.1 for detailed pictures of the 0.5mm case.

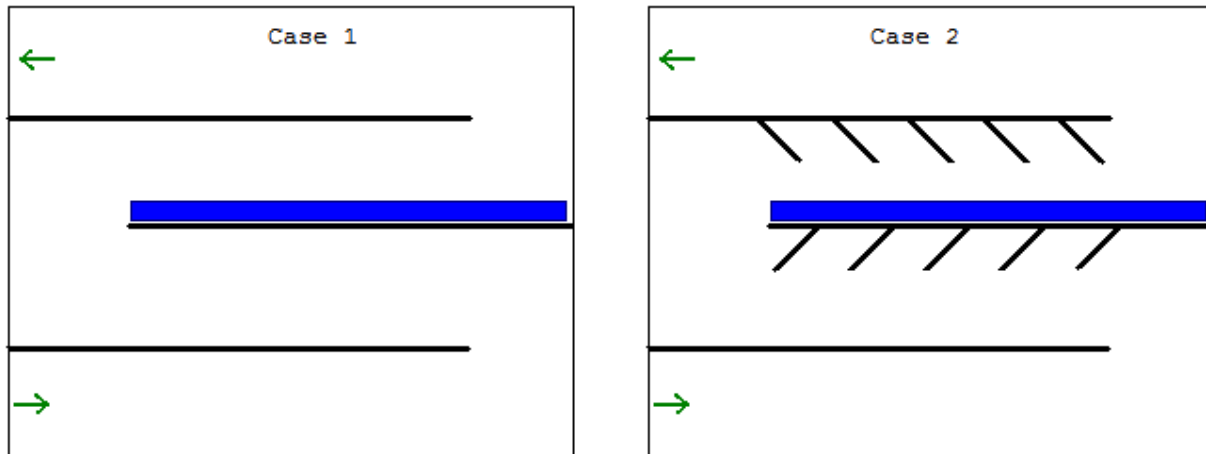
### 5.3 Application – Fruit Dryer

This is a short part presented as an overview, which will show how the constant rate model performed in a more advanced testing environment.

#### 5.3.1 Presentation

The problem of fruit dryer plates is one I am familiar with from an earlier project performed in Yogyakarta, Indonesia. I was there 8 weeks performing fluid dynamics calculations on several setups for a small fruit dryer to find a good alternative for a prototype. However it was impossible at the time to perform any modeling of evaporation and so only heat transfer and flow field calculations were made.

In this short part I will show if the constant rate model could have been a useful tool during this project, and as an example of a possible application. Two dryer geometries will be examined, where the difference between the two will be the type of plates used to place the fruit on.



Pictures 5.2-5.3 – Difference between dryer geometries

Two cases were run, one for each geometry. The above picture describes a cross section of the drying equipment and the differences between the two cases. The objective is to test the model against these two geometries and to see if any conclusions can be drawn concerning the effectiveness of the plate designs. A higher drying rate is preferable, and a good convective flow can possibly accomplish this.

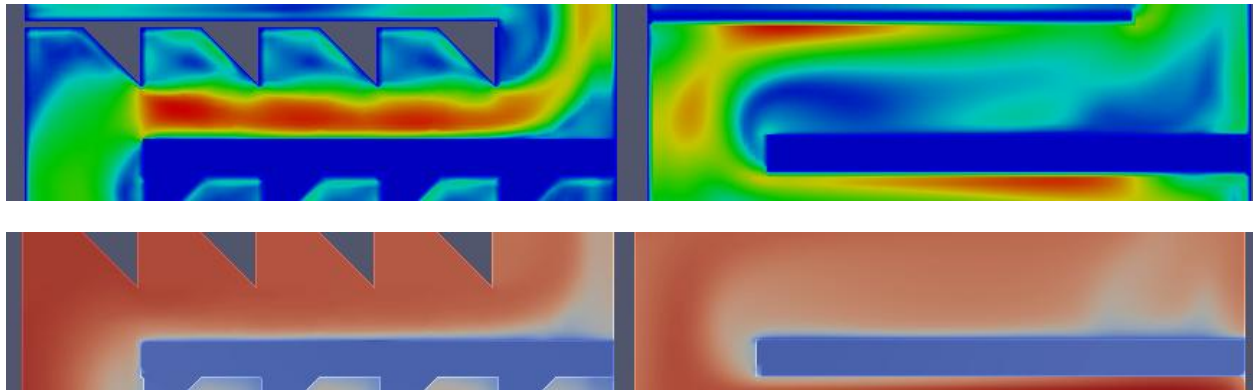
In the first case the heating of the object (blue) will mainly take place from below, by conduction through the plate. In the second case heating must take place from above, since the baffles will hinder any flow close to the plate bottom.

#### 5.3.2 Modelling

The model was enabled for the top surface of the object, and as in the steady state test case this is the only surface where evaporation will occur. Also as for the test case the object will have very high conductivity. This is partly because of the assumptions made, that the object should be at uniform wet temperature and partly because it helps the model converge.



In both cases a boundary layer of an innermost thickness of 0.5mm was used. The first (flat plate) case proved very similar to the test case to run, which is expected because of the similarities in geometry. The second case however proved much more difficult when closing in on the wet temperature of the object. The solver diverged regardless of under-relaxation or other methods as soon as the reaction rate came close to the real value. This was thought to be because of the high convective flow close to the surface.



*Pictures 5.4-5.5 – Simulation data colored by velocity magnitude (top) and temperature (bottom)*

For detailed graphs with scales see appendix A.3.2 & A.3.3.

### 5.3.3 Results

The results for these cases were slightly disappointing, as can be seen below. It was possible to get a good solution for the simple flat plate geometry, which gave a realistic value for the evaporation rate as well. However with the baffled plate case it was not at all possible to reach a converged solution at the reaction rate needed, and the closest possible one still had a  $k_c$  8 times smaller than for the flat plate case. It can be seen from the ‘maximum velocity’ values for the boundary cells that there is not a large difference, thus the high convective flow might not be the problem.

	R <sub>mod</sub>	$k_c$	V <sub>cell</sub>
Units	kg/h		m/s
Flat Plate	0.46	40	0.02
Baffled Plate	0.008	5	0.032

Table 5.2 – Case summary for dryers

The conclusions to be drawn from this are mainly that the constant rate model is able to predict evaporation correctly for simple geometries, but is both unstable and non-flexible. In addition it is likely very difficult to get it working for more complex cases, which is why a new model is needed. As we move on to the falling rate case many of the things learned from the constant rate model will be revisited and developed further. This likely depends on the boundary layer approximation.

## 6. Falling Rate Model

The development of the falling rate model will be based on the discussion in 3.2-3.3 and the continued use of UDF files will allow for a flexible way of dealing with the water content. It has to account for the effects of drying by varying rates over a body due to flow field and temperature conditions, and be able to fit well with measured values.

### 6.0.1 Applications

A model for the falling rate could be combined with the constant rate model to give a more complete model of the whole drying process. Due to the increased complexity it offers more information, such as where drying is most effective, and what effects different flow fields have for the internal conditions of a body. In many processes these are important when designing a dryer, and will allow a screening and testing of ideas before constructing equipment.

This model has potential for further development to deal with bound moisture and with varying diffusivity. By using this work as a base it could be made effective in a broader range of applications.

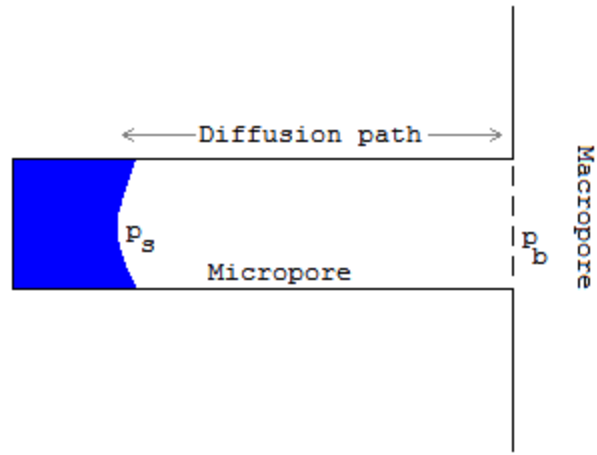
## 6.1 Model Development

### 6.1.1 Assumptions

The main assumption made during the development of this model is that it will deal with a non-shrinking object, a rigid frame. It is further assumed that moisture transport within the material consists solely of vapor diffusion inside the pores, and that the liquid water present does not interact with its surroundings in any other way than the formation of water vapor and consumption of heat. Depending on the settings the liquid water content will influence some chosen variables in the model, however.

Since the actual formation of vapor should be similar to that of free water, a similar expression as in the constant rate model for the formation of water is used. The difference is that the source term is bound to the whole material and will make sure that as long as there is liquid water in a region, the vapor in the gas phase will be saturated at the liquid interface. The liquid interface is handled the same way as in the first model, by a fictive surface exerting its maximum vapor pressure on the surroundings. One might imagine a liquid surface inside a small pore, with saturated vapor directly above it, which will diffuse outwards.

Since the object chosen is simple with respect to common materials being dried, such as fruit, we can omit a number of factors. We do not need to consider equilibrium moisture content, since there is no bound water, and the diffusivity can be taken as constant since there is only diffusion in large channels. However these additions would be easy to create.



Picture 6.1 – Assumed behavior of water in porous material

### 6.1.2 Expressions

The reaction rate of water will be found from a similar expression like Eq 3.12. Since the  $K_c$  values were found to differ a great extent from 1 in the constant rate case it has been streamlined and it is assumed that much of the calibration has to be done with the  $K_c$  constant. Another difference is that this expression now represents diffusion from a water surface inside the channels of the materials and that it is applied to the cell volume directly, instead of a surface. See picture 6.1 above.

$$\text{---} \quad \text{---} \quad (6.1)$$

To track the water content of the object being dried, a normalized water content is introduced. It is simply a constant in the range [0 1] where 1 represents the starting water content. This property can be related to the moisture content by:

$$\text{---} \quad (6.2)$$

Where  $W_s$  is the solid density and  $W_{w,start}$  is the starting water content. Both are defined in  $\text{kg}/\text{m}^3$ . is used to keep track of the water content and to estimate the changing material properties of the material. The density of the solid material is defined by:

$$(6.3)$$

Thus the water is considered to be packed within the solid material in this model, and will alter the values of the material as it drops off. The conductivity of the material is defined in a similar way by mass weighing:

$$\text{---} \quad (6.4)$$

Unfortunately it was not possible to alter the heat capacity values in a similar way, due to lack of that function when writing fluent UDFs. They could only be altered with a temperature function.

The diffusivity inside the body will be different from that in the bulk gas. To account for this it will be set to a lower value with the UDF file for all body cells. A function will be implemented to do this. The base

diffusivity is calculated from the expression in Appendix A.1 or set to the normal value of  $2.88e-5$  depending on need.

### 6.1.3 Limitations & Problems

The main limitation of this model is the way that liquid water is described. Since the water is modeled indirectly the model will need to account for the important interphase interactions without actually resolving liquid water in Fluent. Features such as capillary movement and liquid diffusion cannot be modeled directly with this method, but it is possible that the phenomena can be described by changing involved parameters in such a way that it fits with experiments.

The model is dependent on the porous medium formulation in fluent, which assumes isotropic conditions inside a material and weights many parameters between solid and bulk phases.

### 6.1.4 Geometry and Boundary Conditions

The domain that will be used to test the initial model will, as in the steady state case, be quite simple. It is reasonable to assume that the start of the falling rate period will show similarities to the constant rate case. If this holds, and the expected behaviors of the falling rate period can be observed, then the model can be deemed functional and be tested against a more advanced case.

Thus the geometry will be the same as in the constant rate case, with the exception that the solid plate is now modeled as a porous zone to which the water will be attached. The porous cells will be loaded with  $20 \text{ kg H}_2\text{O per m}^3$ . For the whole plate this is  $0.3 \text{ kg liquid water}$ .

## 6.2 Modeling

The first objective when using the falling rate model is to initiate the flow field to find a good starting field. When patching in the water content and running the model normally several non-physical things will happen, first there will be a huge reaction rate since there is no water vapor inside the porous body. This will result in a large overestimation of the initial reaction rate. Second the water will diffuse out of the body with great speed due to the newly formed concentration gradient, which is very large at this point. This effect increases with temperature, because of the saturation pressure dependence on temperature. A monitor should be enabled to observe the reaction rate.

If monitoring the reaction rate and water formation one will see a large spike of water quickly after starting the modeling run. Since this is a non-physical side effect of the model formulation one needs to disable the adjustment of  $\epsilon$  so that no reacting water is drawn from the stored water in the body. Then the simulation will need to run until the flow field is completely stable, and the reaction rate is constant. This may very well take a while, since the formation of concentration profiles inside the porous body will depend a lot on which diffusivity values are entered. If changing the reaction rate constant or other values this will need to be done again, thus being a time demanding process. Once a steady state solution is reached one may check that it corresponds to a correlation or experimental value, correctly describing the situation to be modeled. Once these settings are done the  $\epsilon$  adjustment should be enabled, to let the reaction deplete the stored liquid water.

At this stage it may be wise to enable some extra monitors to keep track of things such as , temperatures and exiting vapor. Also if need be enabling auto saving of data at certain time intervals. Now the simulation will run, depleting the water stored in cells and drying the body(ies). At first the reaction rate will remain constant, since there is no internal resistance to diffusion at the surface of the body. As soon as the surface cells are emptied however, the water will retreat beyond the surface and the rate will start to drop off. The behavior of this period will be strongly affected by the geometry, flow field and diffusivity. Depending on the mesh detail of the porous body the rate may fall off in a step-function like manner. To correctly depict the falling rate behavior the body should have a sufficiently detailed mesh.

Using the falling rate model proved to be easier and more forgiving than using the constant rate model. Since the velocities inside the porous body will (in most cases) be very close to zero the diffusion film assumption holds better in this case. In most cases the reaction rate will not be the limiting factor when the water content has retreated below the surface, since the process is often controlled by internal diffusion at this stage. A drawback of this model is the long times needed to initiate the flow field, but differing from the constant rate model working with this model do not require manual adjustments while running. In addition it can be used to model constant rate behavior as well, since one need not enable the adjustment function.

Pictures of the starting state of the first run can be found in appendix A.3.4.

### 6.2.1 Case Results

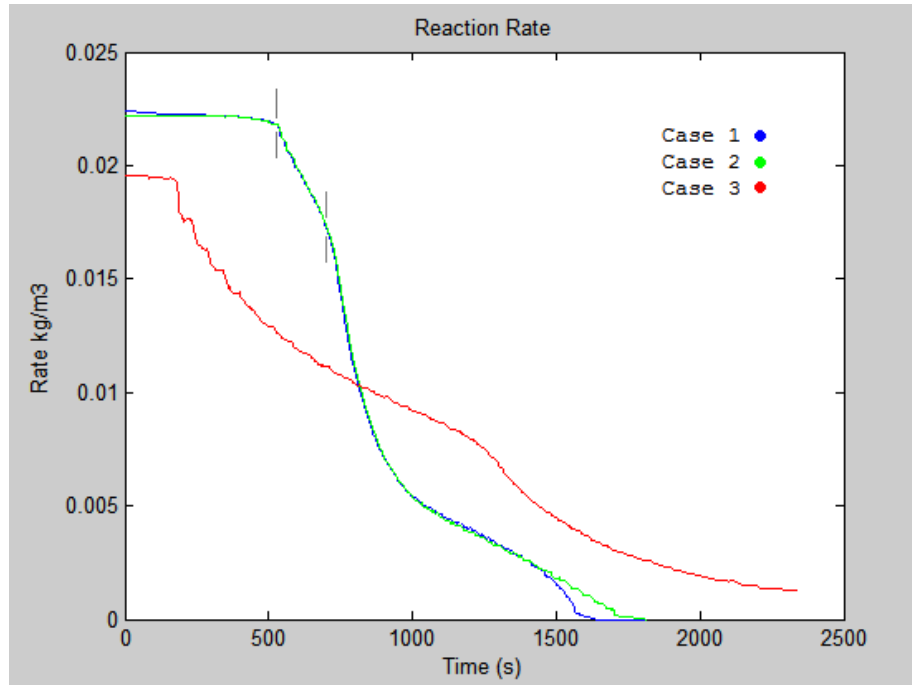
Three different cases were run. The differences between them are presented in the table below. The porous material was loaded with 20 kg/m<sup>3</sup> liquid water and the porous material treated as cordite. The cases were not adjusted so that the rate corresponded to reality since the sought after information was in the behavior of the drying, to which using an arbitrary reaction rate is no problem. The parameter changed is the diffusivity of vapor inside the porous material to see what effects can be observed in the drying. Other values such as inlet temperature were the same as in the constant rate runs.

For the first case the diffusivity in the porous material was given a constant value of 100% of the value in air. For the second case, a value of 5% was used. For the third case, the diffusivity was weighted against the water loading of the material so that a cell which is full will have a very low diffusivity, while an emptied cell has the value of air. The equation is presented below, and chosen so that there will be a remarkable effect in diffusivity when a cell starts emptying. For the final case the effect of a changed reaction rate constant was examined.

$$(6.5)$$

We can see a number of interesting things in the graph presented below. The reaction rates of the various cases are plotted against time. Case 1 (blue) and Case 2 (green) show remarkable similarities. The effect of the change in diffusivity is clearly not visible, so a value of 5% was likely still too high to have an effect. There is a small effect at the end, where the green rate takes slightly longer to drop off. However in both these graphs the behavior of the drying periods can be clearly observed. They start off with a constant rate period, where we have evaporation from a surface, and enter the first falling rate

period after that. This behavior is visible for a short while until a long second falling rate period is entered. The periods are divided by grey dashes in the diagram.

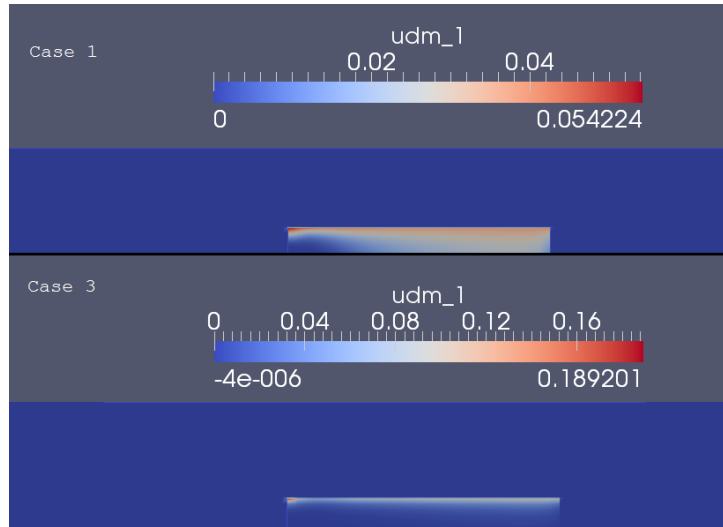


Picture 6.2 – Reaction rate Vs time for three test cases

As the geometry chosen should not present this type of behavior this may seem strange, but it is an effect of the reaction rate and the reason can be observed in pictures below, of the reaction rate in different parts of the geometry. An oval part at one edge of the plate is left when most water has evaporated, which will give a behavior similar to diffusion out from a spherical object. This has the pleasant side effect of showing the potential of the model for modeling this type of behavior. For the third case (red) we can see a steady drop-off effect due to the weighing equation which negates the effect above and provides a more even reaction rate as cells are emptied sequentially.

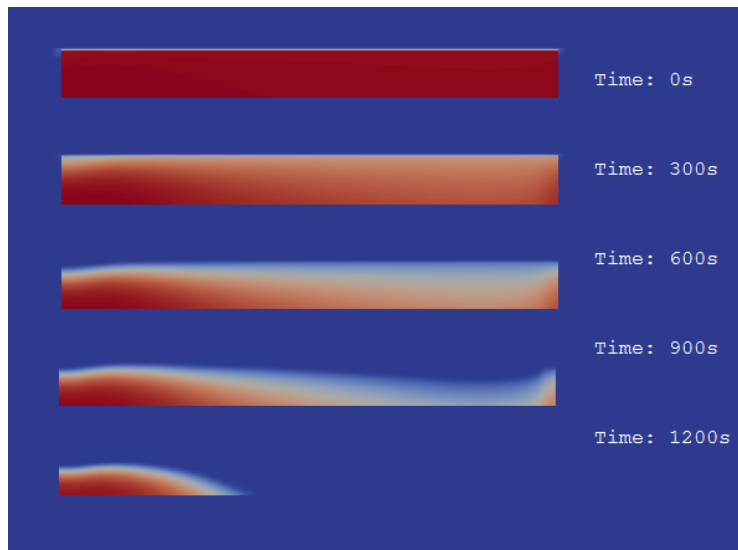
One can see step-like behavior in the graph for the third case, which shows that the mesh is not detailed enough since the emptying of one cell will provide a large increase in resistance when water needs to diffuse from the next. This type of behavior can be seen in the other graphs as well, most notably during the last stages of the green graph.

From this we can conclude that the model will likely be able to cover a wide range of setups and rate drop-offs, depending on the need of the user. The adjustment can be made primarily with changes to diffusivity and reaction rate, but material properties will have an effect as well.



Picture 6.3 – Starting reaction rates in the geometry for Cases 1 and 3

The above picture describes the reaction rate (UDM 1) in various parts of the geometry at the start of the run. The cases 1 and 2 are very similar, like for the rate curves. However the third case clearly shows that water is forming only at the surface of the object. This explains the slightly lower reaction rate, as well as the gradual drop-off behavior compared to the other two cases.



Picture 6.4 – Water content at different simulation times

The above picture shows the value of the normalized water content varying over time for case 1. In the first picture the water content has been patched in, providing a value of 1 to the whole material. Gradually drops off, leaving the oval part at the bottom clearly visible. It is this behavior that leads to the second-falling rate period behavior of the rate graphs above.

In an organic material it should be possible to lower the diffusivity to model diffusing liquid. Model shows general falling rate behavior and realistic values.

### 6.3 Application – Drying of Catalyst

This part presents the application of the falling rate model on an advanced case, and will not go into detail on all aspects of the modeling since this would take a lot of time and space.

This simulation was used in the result of an article by Andreas Lundström at Kemisk Reaktionsteknik (Chemical Reaction Engineering), Chalmers. Experimental data provided by Andreas is used in the validation of the results.

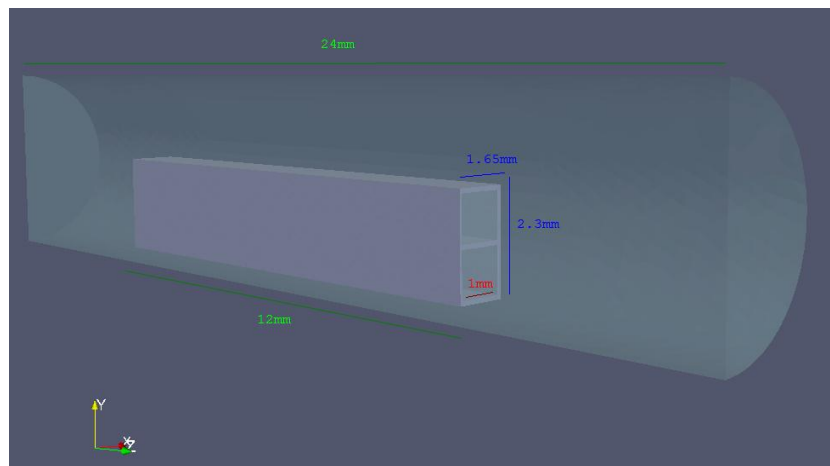
#### 6.3.1 Presentation

As an applied case for the falling rate model, a complex mesh and advanced problem will be presented and solved. The problem consists of the modeling of water evaporation from a porous catalyst body. The piece of catalyst is very small and contains four channels. It is located in a small pipe where air flows, surrounding it. The material of the catalyst is cordite, as for the test case. The problem will require a highly detailed mesh, and a symmetry plane will allow for modeling only half of the actual pipe. The mesh is presented below.

The air flowing into the domain and the surrounding walls will be gradually heated according to the following temperature ramp function, where  $T_0=293$  K and  $t$  is the time in seconds. The ramp will start at 293K and the experiment will end at roughly 390K.

$$- \quad (6.6)$$

Measurements will be done with monitors enabled to keep track of the heat loss due to evaporation, this will be compared to experimental data to test the validity of the modeling. The inlet air flows with a velocity of 0.063 m/s, and a temperature decided by the temperature ramp function. The time step used was 0.25s although several intervals were tested to show time step independence. The inlet air had an initial moisture content. It was set to a mass fraction of 1.5%, the conditions under which the experiment was performed.



Picture 6.5 – Catalyst case geometry, using symmetry plane



### 6.3.2 Modeling

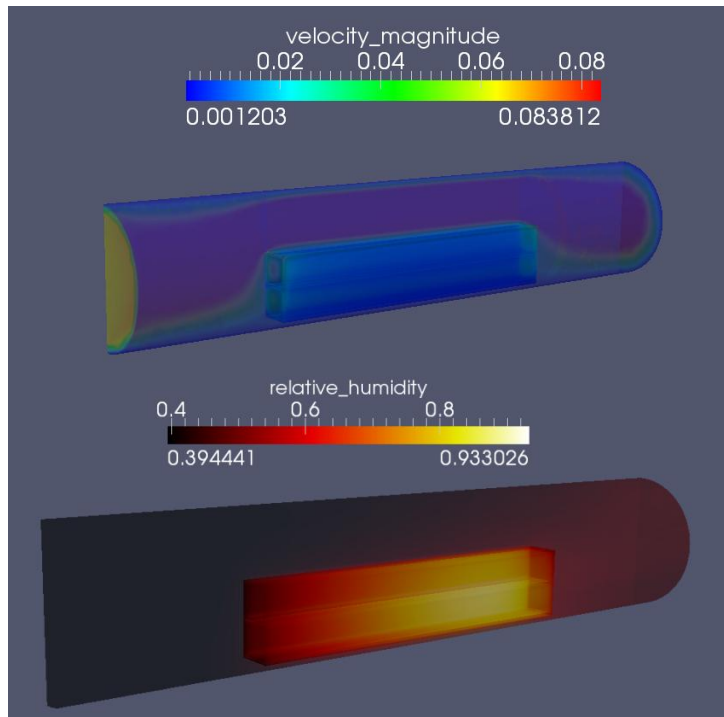
The objective of the simulation is to match, as closely as possible, the model results to that of the experimental data. The data is given as the heat flux from the wall region, and will be used to adjust model parameters to fit the curve. The information required is mainly the examination of assumptions made by Andreas Lundström in the development of a 1D model for this case in his article. The main assumption is that the heat flux from the wall is a very large contributor to the heat of the evaporation, and that the other source, convective transfer from inlet, can be ignored for modeling purposes. It is also of interest to study the general behavior of the process.

The modeling made use of the falling rate model developed above, and included the temperature ramp in the UDF for use as a boundary condition for walls and inlet. For a summary of the use of the UDF see appendix A.2.2. Since the temperature ramp was used, and the scale of the problem is quite small it would not behave like the typical falling rate periods described above. This is mainly because the distance for diffusion is so small but also of course the irregular geometry.

The application of the falling rate model to this case is appropriate since the catalyst is a porous object with a rigid frame, fitting the assumptions made during the model development. The case was set up and the run basically followed the process described in 6.2. Several monitors were used, among the most important were the heat flux from the wall and UDM 0 ( ).

For each run a number of curves were obtained, which allowed comparison to the experimental data and adjustments. An iterative process was used to find the correct values of variables in the model of which the most interesting were:  $k_c$  the reaction rate constant and  $D$ , the diffusivity in the porous material. Other variables adjusted were material properties of the catalyst material, since they will be influenced by the water amount left, .

It was found that the most important parameter was  $k_c$  (from 6.1) obtaining a final value of 3.7. Because of the small diffusion distances the process was not diffusion limited to a normal extent and the reaction rate took precedence. The diffusivity was adjusted from its original value of 100% of the diffusivity in air, down to 1%. This had very little effect on the reaction rate curve or other values. Values determining catalyst conductivity and density were initially set as constant, for the sake of simplicity. Changing these material properties to use the weighing functions described in the development of the falling rate model gave a slightly better fit.



Picture 6.6 – Simulation data colored by velocity magnitude (top) and water vapor (bottom) for  $t=100s$

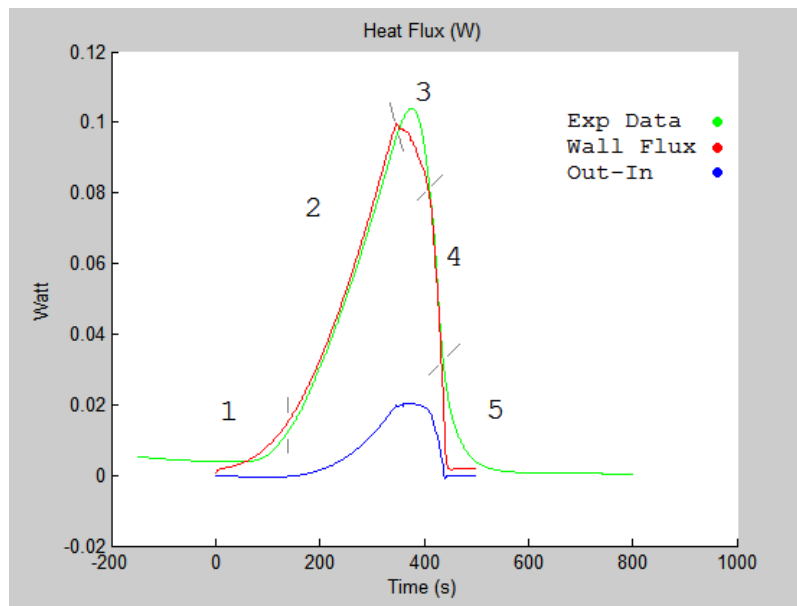
The air passed mostly past the catalyst object, although a low velocity can be observed in the channels, transporting water vapor and cool air out of the catalyst. Since the walls provide heat for the evaporation process, the object will show an irregular reaction rate due to some parts closer to the wall being heated first, and also emptying first.

There were some problems encountered during the simulation runs on this case, but they were mostly related to mistakes made in the UDF code, and once the UDF was fixed the modeling proved to be easy and without numerical issues or otherwise non-physical problems. In addition the curves for heat flux and reaction rate were smooth, and did not show the amount of mesh-dependent step-like behavior observed in the results for the test case above. An interesting thing to note is that condensation was clearly observed during the short preheating period, increasing the value of  $\phi$  slightly above 1, before the temperature was high enough to start evaporation.

Once the correct parameters had been found, the overall time for the simulation came in at 500 seconds with all water gone at 450 seconds. Data for the simulation at three time intervals can be seen in appendix A.3.6-A.3.8 for times 100, 350 and 425 seconds.

### 6.3.3 Results

The results were overall surprisingly positive. Once the model parameters were fitted to the experimental data the model was found to describe the experiment very well in general. For comparison the graph for heat flux was used, and the result can be seen in the picture below. Two main periods for the drying can be observed, we can call them period 2 and 4 respectively. Period 2 allows free evaporation from the whole catalyst, and the value of  $\theta$ , the water content is non-zero in all cells. During this period the reaction rate is controlled by the total heat flux to the material. In period 4 the water content is gradually becoming zero in the material, which results in a sharply decreasing reaction rate due to less volume available for the evaporation. The controlling mechanism for this period ought to be the geometry itself. The model was able to follow these two periods very well, but the three short periods not in the main periods show differing behaviour.

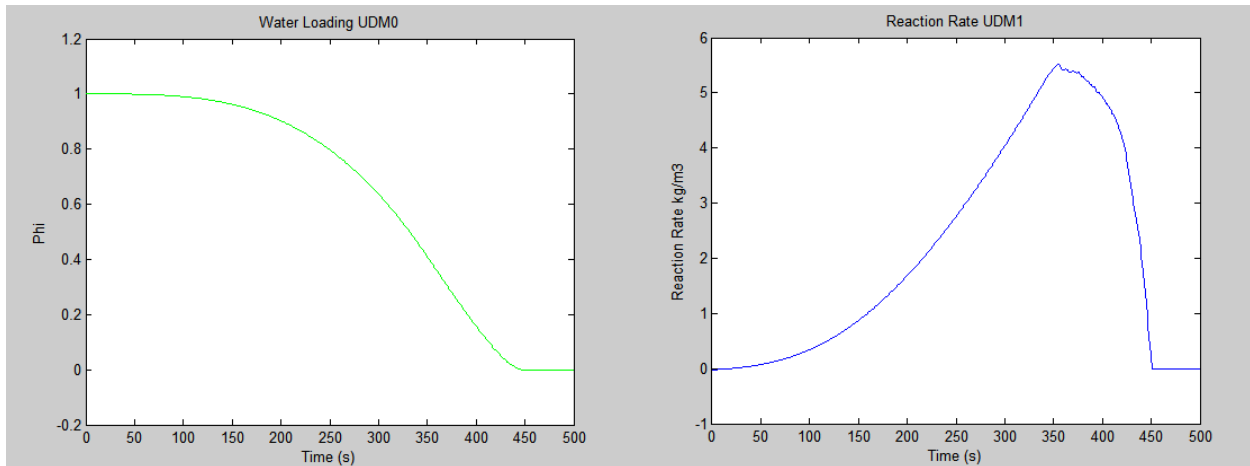


Picture 6.7 – Heat flux graphs and experimental data

For period 1 it is unclear why the model diverges from the experiment, but a likely cause is that the starting conditions and startup differs somewhat. It can be seen that the starting heat flux initially differs between the experiment and the model, and it could be a question of initial temperature, or the behavior of the temperature ramp. It is also possible that this period is not modeled with the correct  $C_p$  value, since this material constant could not be weighted like the conductivity and density, and that this period pre-heats the material which makes it depend on  $C_p$ .

Period 3 shows an irregularity in behavior with an initial sharp drop-off in reaction rate. One can see that the initial emptying of the first cell has an immediate effect on the rate. Where in reality the emptying would be gradual, the model treats it as instant. This effect could be because of the simplicity of the porous media formulation as well as the model not treating adsorption heat. This could be changed and tested, and can hopefully be corrected in future use of this model.

Period 5 shows a more gradual drop-off behavior for the experiment, likely this depends on two things; they are basically the same as for period 3, in reality the final emptying is gradual instead of instant and probably requires additional heat since the water is surface adsorbed. It could also be because of the porous media formulation, where the last stages in reality could be diffusion limited. Since the water is contained in small pores where diffusion could be a limiting factor, it is possible to correct this slightly by lowering the diffusion. This was done in the modeling but did not have a major effect in this case, so it was omitted. Function dependant diffusivity, like for the test case, could possibly fix this.



Picture 6.8 – Water content and reaction rate Vs time

By observing the above graphs for the value of  $\Phi$  and the reaction rate, and comparing with the pictures in appendix A.3.6-A.3.8 several of the effects discussed above can be observed. We can see that the reaction rate above is very similar to the wall heat flux curve, as expected.

What about the conclusions then? We can see that the question asked about the wall heat flux controlling the process is answered. The heat contribution from the inlet grows with temperature, but is never dominant and during most of the process very small. However it has a sizeable contribution at the reaction rate peak and it can probably not be ignored completely for the sake of a 1D mathematical model. Of course this depends on the level of detail required.

The model performance is deemed good for this quite complex case, which shows it can probably be used for a wide range of conditions and applications. It clearly has possibilities for improvement though, and the most interesting ones are the addition of adsorption heat and using diffusivity functions to compensate for the porous media formulation. If it is possible to find a solution to the  $C_p$  weighing with this would be of use as well.

## 6. Discussion & Conclusions

The problems listed in the problem description consisted of time scales, phase interaction and different periods of drying behavior. The problem of *time scales* was solved by not treating the evaporation and condensation reactions separately but instead solving an equation for their sum, the total reaction rate. This was done by using the film diffusion concept and a number of assumptions. Doing this reduced the spectrum of time scales, and for the falling rate model this ended up working well. The *phase interaction* was not treated directly in the CFD simulation which made it possible to use only gas in the simulation. It was treated as perfectly bound to the material, and an external source kept track of this value in the UDF. This made it possible to weigh several material properties so as to have the stationary water interact with the solver indirectly. Finally the *periods of drying* showed themselves as a result of the assumptions made in the model and using the falling rate model one may describe the constant rate period as well as preheating period and the several falling rate periods.

The model in its current state has a wide number of *applications* including materials of type I, like clay and porous materials that do not contain bound moisture. Thus it can be used for drying of most ceramics, and also for a bed of small objects, like small fruit pieces. It should be possible to deal with most objects that do not shrink, or shrink very little during drying. Perhaps it is even possible to use it for shrinking objects with a few simplifications, but the results could well prove inaccurate. Only testing will show how it holds up to these situations.

The *shortcomings* of the model at the moment consist mainly of its dependence on the user to specify what types of interactions occur between the bound water and the simulation. It is also not possible to have the liquid water move from its position in since it is treated as perfectly stationary. Thus it needs to be used in situations where this assumption holds. The model is dependent on the porous medium formulation in Fluent, which may prove difficult if one wants to use it for non-uniform materials like wood fibers, where the diffusivity varies with direction.

There are several possibilities for *further development* of the falling rate model. As it stands now it is able to model evaporation from solid porous objects, with a rigid frame. To expand the possibilities of it would be to make it able to handle objects with changing diffusivity and/or low diffusivity compared to vapor diffusion. This would include the need of modeling liquid diffusion in fluent, which could very well be a complex situation if intending to use one-phase modeling. Perhaps it would be possible to include an additional reaction step that is liquid water in between the bound water and the vapor. Objects such as fruit will require the addition of changing adsorption heat and the equilibrium moisture content effect. This could be done in a few steps from the current model. A way for dealing with a shrinking object would be difficult to do, and would be best modeled by a function dependant diffusivity.

## References

- [1] Drying of loose and particulate materials, *R. B. Keey*
- [2] Albright's Chemical Engineering Handbook, *Lyle F Albright*
- [3] Separation process principles, 2<sup>nd</sup>. *J. D Seader, Ernest J Henley*
- [4] Computational Fluid Dynamics for chemical engineers, *B. Andersson, R.Andersson, L.Håkansson, M.Mortensen, R. Sudiyo, B. van Wachem*
- [5] Mass transfer fundamentals and applications, *Anthony L. Hines, Robert N. Maddox*
- [6] CFD Modeling of the heat and mass transfer process during the evaporation from a circular cylinder, *Fransisco J. Trujillo, Simon J. Lovatt, Mark B. Harris, Jim Willix, Q. Tuan Pham*
- [7] Fluent 6.3 UDF Manual
- [8] Modeling local heat and mass transfer in food slabs due to air jet impingement, *M.V. De Bonis, G. Ruocco*
- [9] Expressions for predicting liquid evaporation flux: Statistical rate theory approach, *C.A. Ward, G. Fang*
- [10] Drying kinetics of water based ceramic suspensions for tape casting, *B.J. Briscoe, G.Lo. Biundo, N. Özkan*
- [11] Drying characteristics and kinetics of coffee berry, *P.C. Correa, O. Resende, D.M. Ribiero*

## Appendix

### A.1 Relations

#### Goff-Gratch approximation for water vapor pressure

$P^o$  is the saturation pressure (hPa)

$P_b^o$  is the saturation pressure at 1atm and 100 °c (1013.25 hPa)

$T_b$  is the boiling point temperature (373.15 K)

$T$  is the air temperature (K)

#### Diffusivity of vapor expression in air (Bolz and Tuve )

$T$  in Kelvin

## A.2 UDF Files

### A.2.1 Presentation of UDF - Constant Rate

The function used to model the reaction of water is written as a source term for fluent, which can be enabled for a flow region. It needs to be compiled and requires some user inputs. The source term should be applied in the flow region that borders to the surface where evaporation will occur, that is not to the surface or body. This is because it needs data from adjacent surface cells. To use the UDF the user should:

- Find the ID of the surface thread that corresponds to the evaporation surface in the fluent panel.
- Enable one user-defined memory location (UDMI).
- Open the UDF file and input the ID number into the 'fThreadID' variable.
- Enter the species number for water in fluent (0, 1, 2 etc.) which depends on where water is placed in the mixture model panel.
- Enter a low number of the factor  $k_c$  ( $\sim 1$ )
- Compile the UDF and apply source terms for water and energy to the fluid zone.

The UDF is treated as a source term, meaning it will be called from all cells in the fluid region. A loop within the UDF checks all the surfaces of the current cell, and if one of those surfaces corresponds to the given ID, it is identified as a surface where evaporation will occur and the program continues. Otherwise the source term is given as zero.

The program will find the location of the surface and the central node of the cell and create a fictive boundary layer distance between them. The vapor concentration in the cell is taken as the bulk concentration, and the vapor concentration at the surface is set to that of the saturation vapor pressure at the current temperature.

The name of the UDF is CR-Final.c and is included in the report package.



### A.2.2. Presentation of UDF – Falling Rate

The function used to model the falling rate period is written as a source term for a fluid region, most likely a porous region. It needs to be compiled and requires some user inputs. Many material data are inserted in the UDF instead of fluent, and several variables need to be set. The basic process to use the UDF is as follows

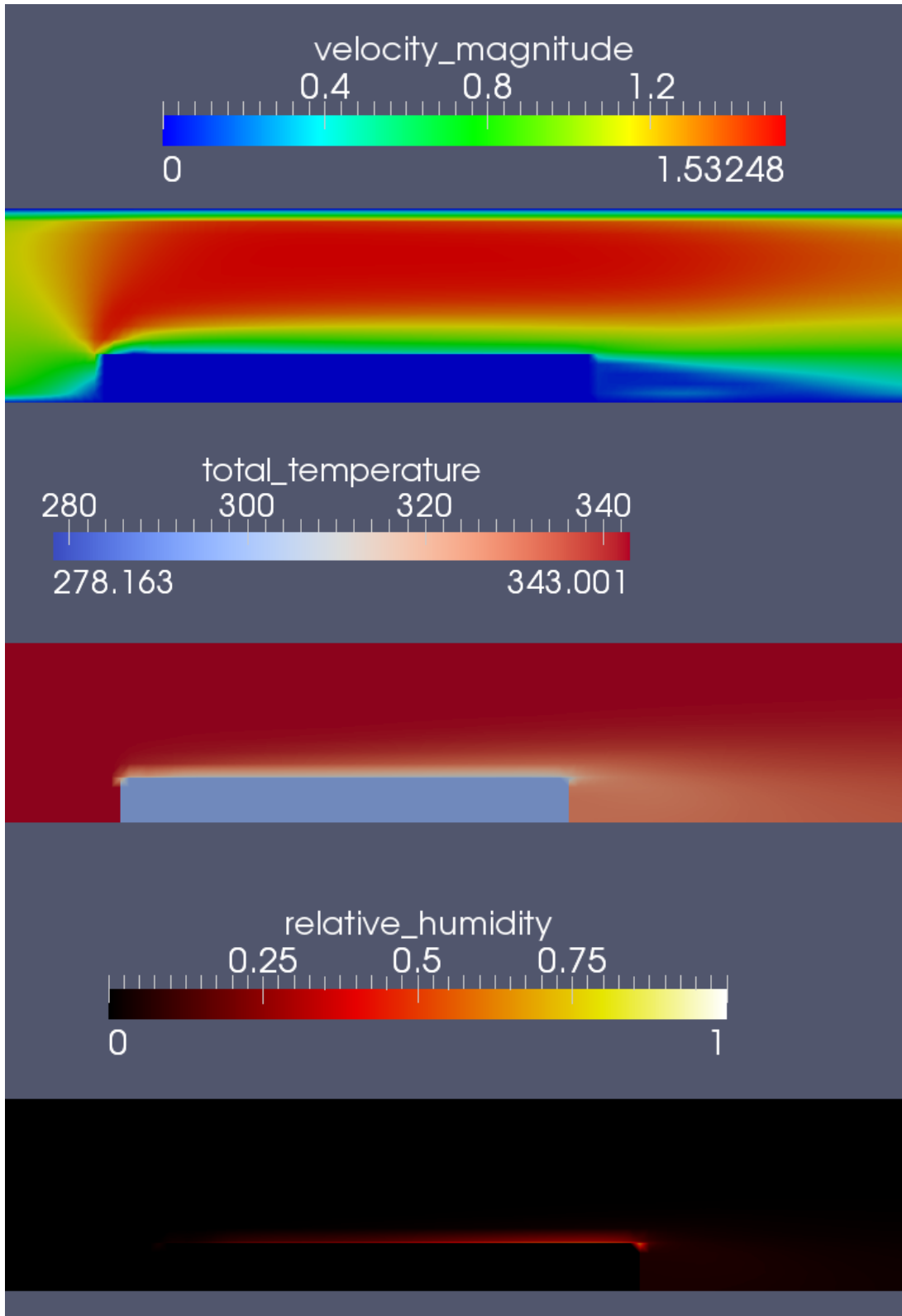
- Find the ID of the cell thread corresponding to the porous region from the panel in fluent.
- Enable three user-defined memory locations (UDMI).
- Open the UDF file and input the ID number into the POROUS\_ID variable.
- Check so that the species in the UDF correspond to the species chosen in fluent.
- Enter values for  $k_c$ , water loading, and material properties.
- If wishing to modify the diffusivity in the porous region, check and modify the expression on line 138, otherwise set it as  $D_{ab}$ .
- Compile the UDF and apply the source term to the porous region. Apply the material property functions to the porous material if they are to be used.
- Initialize the case, and patch a value of 1 to UDM 0. Enable a monitor for UDM 1.
- Run the case until steady state is reached.
- Enable phi adjustment in the function hook panel and any monitors and data file saving.
- Run the case and water will evaporate.

The UDF is called from all cells within the porous zone, where evaporation will occur if UDM 0 (phi) is not 0. If phi adjustment is enabled the evaporated water will be removed from UDM 0, and the zone gradually depleted. The reaction rate will depend on  $k_c$  and the temperature.

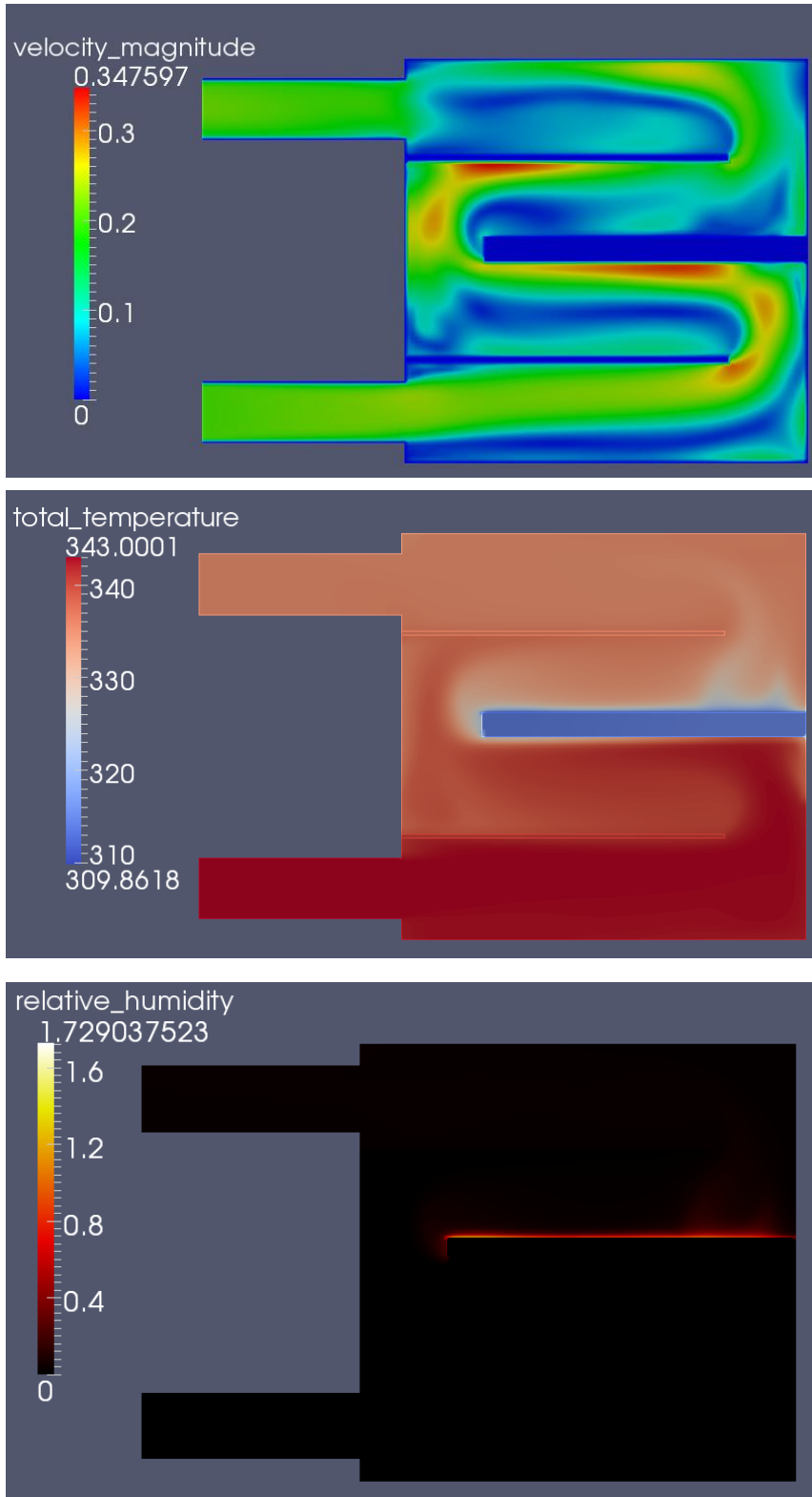
The name of the UDF is FR-Final.c and is included in the report package.

### A.3. Pretty Pictures

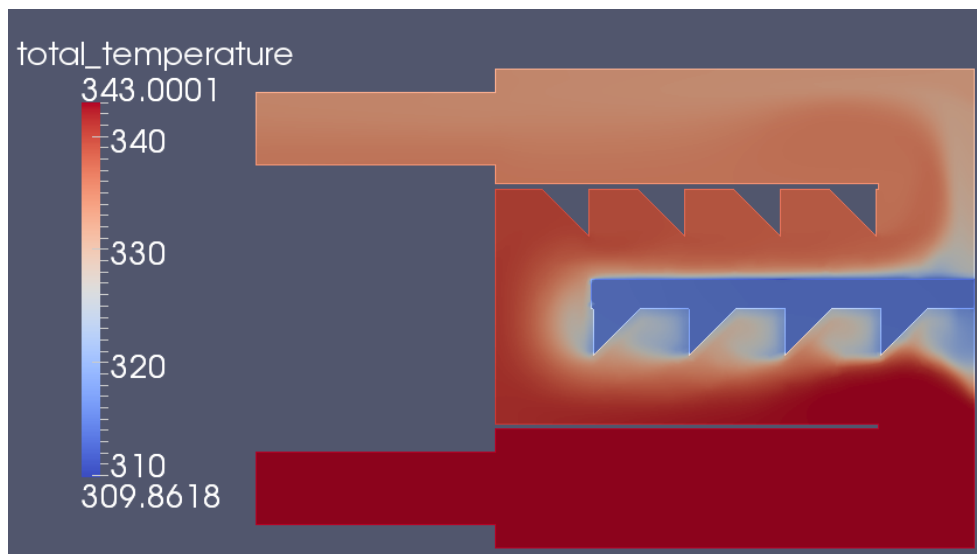
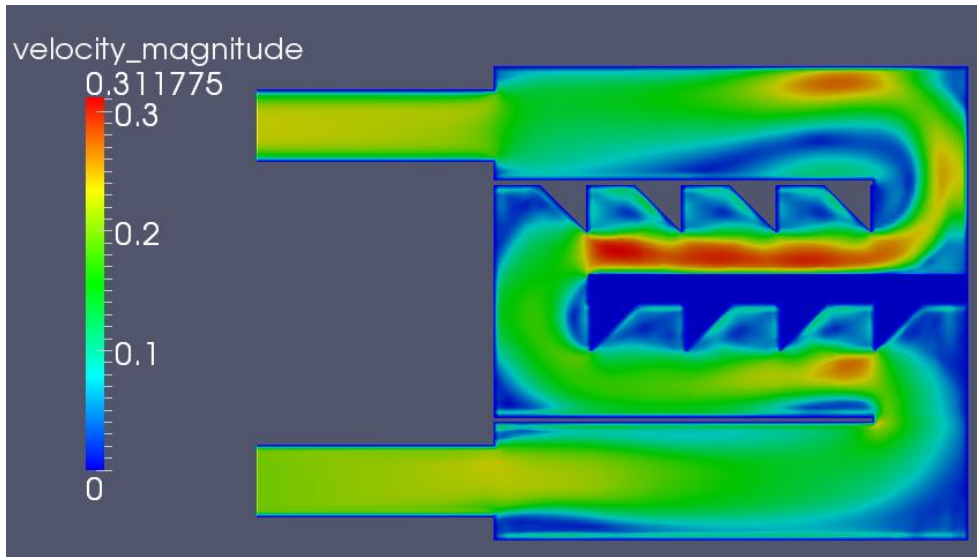
#### A.3.1 Test Case Constant Rate



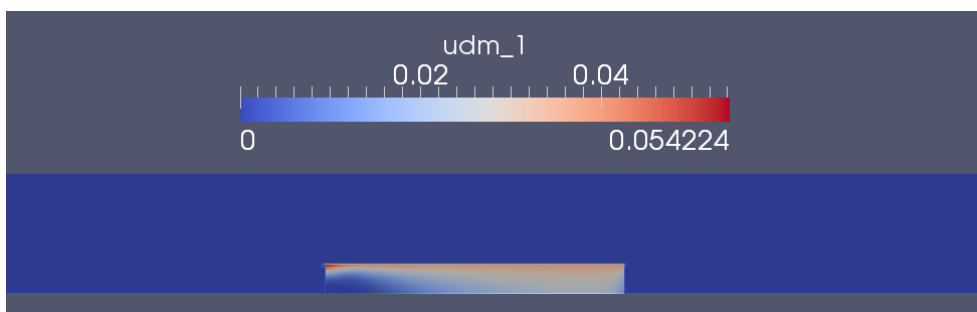
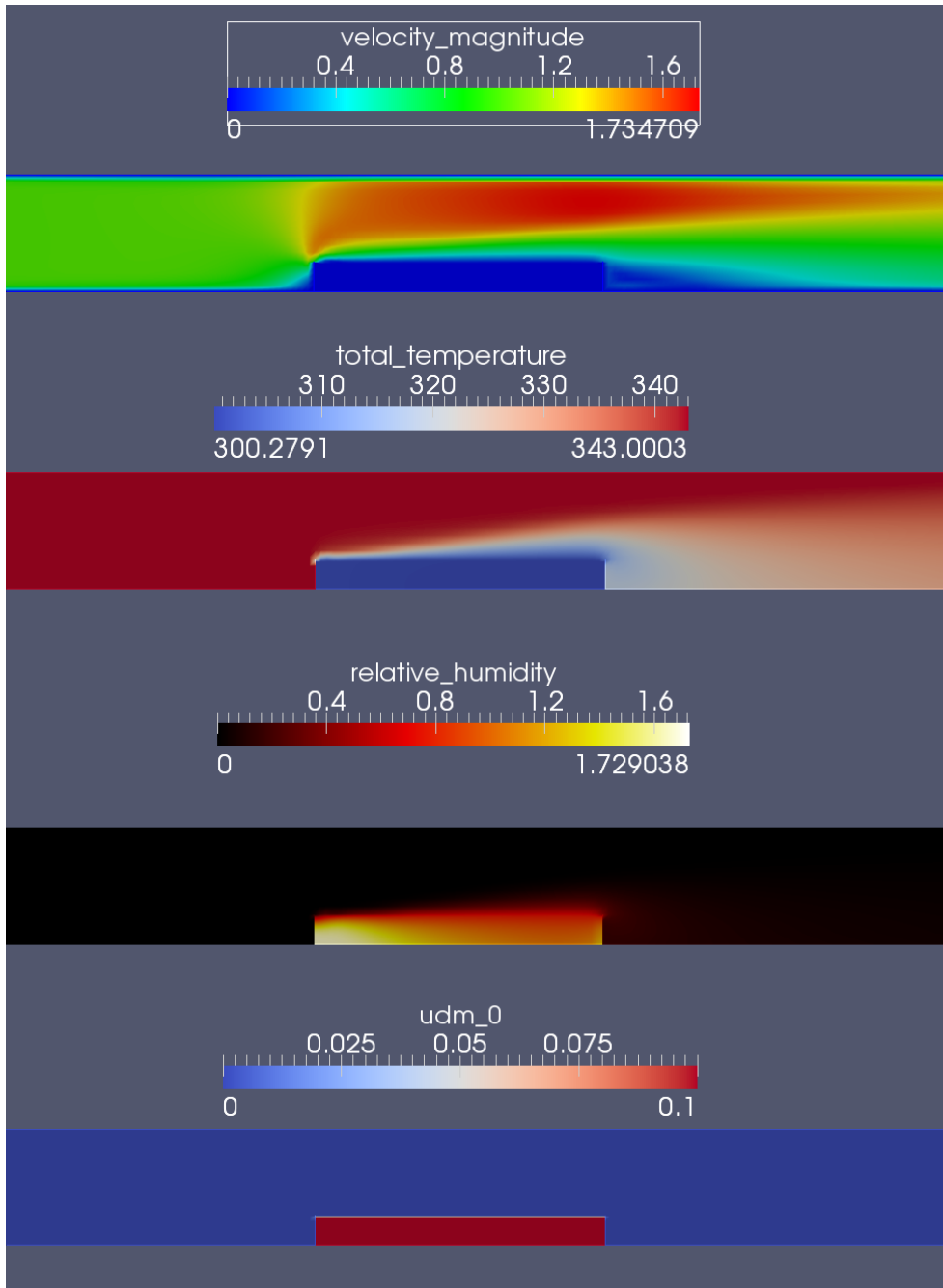
### A.3.2 Dryer Plate Case



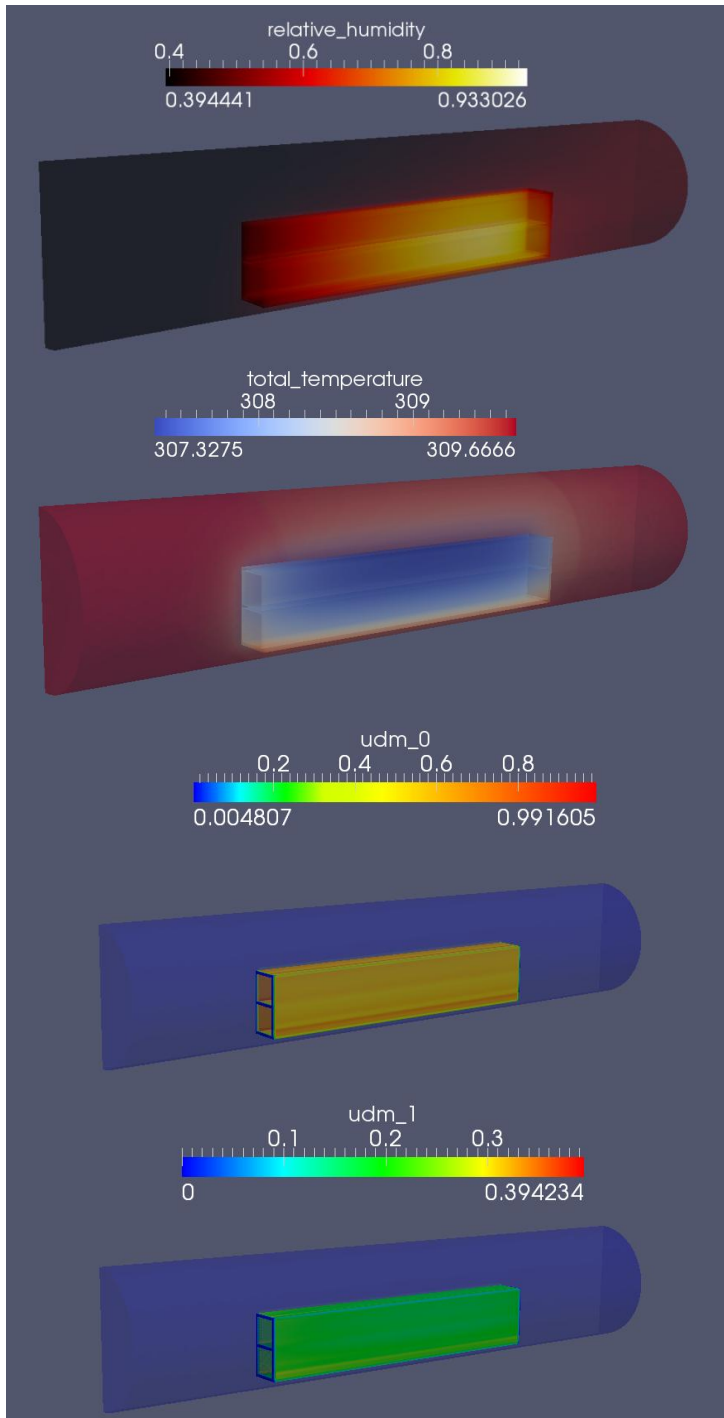
### A.3.3 Dryer Baffled Case



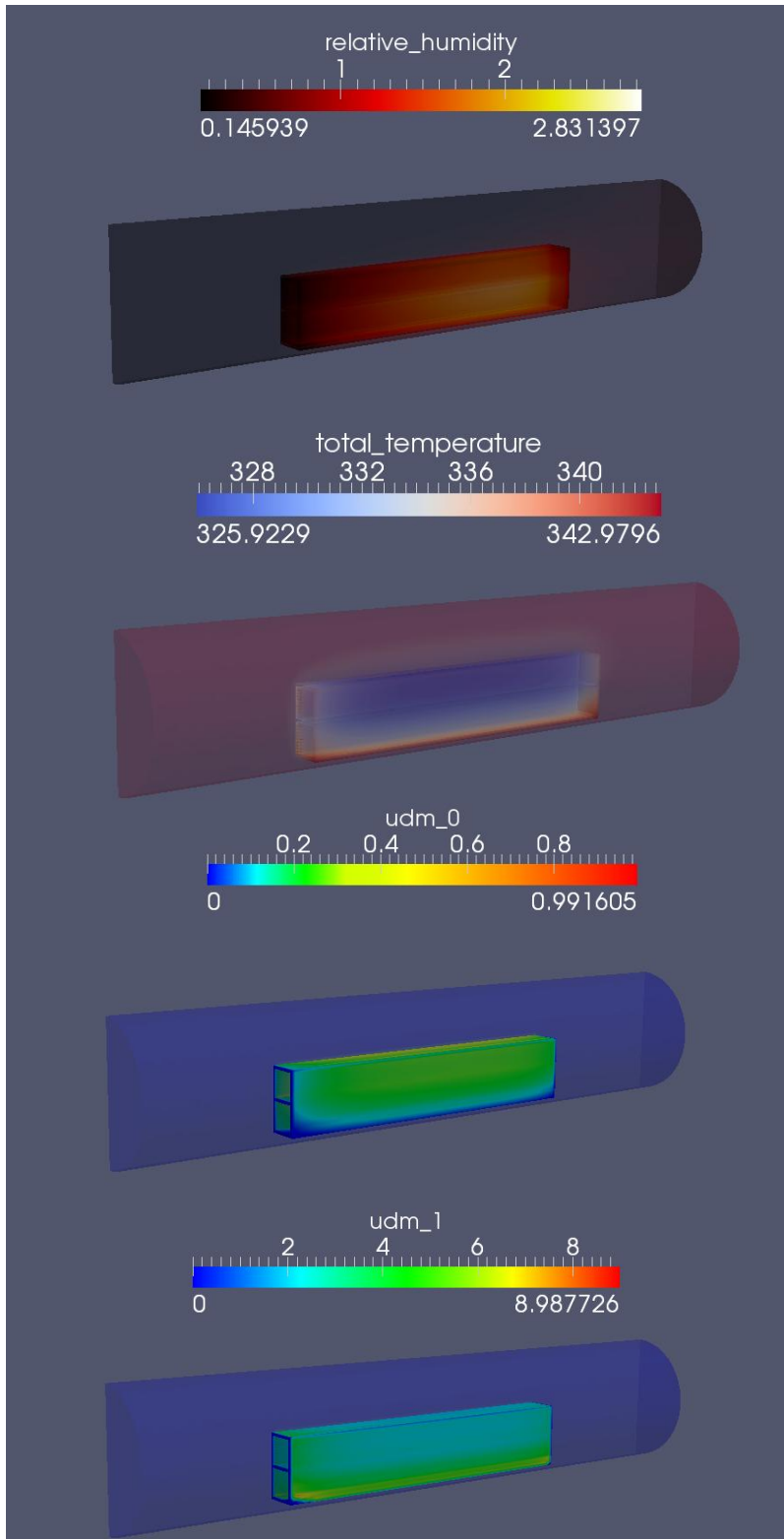
### A.3.4 Falling Rate Test Case – Startup



### A.3.6 Catalyst - 100s



### A.3.6 Catalyst - 350s



### A.3.7 Catalyst - 425s

